THE DEVELOPMENT OF POLYMER-ZEOLITE COMPOSITE AS A MOLECULAR SIEVE FOR WATER REMOVAL IN BIO-ETHANOL

KHEMMARAT WANNAMAHINTRA
ARIYACHAI MANEESAI

A SPECIAL PROJECT SUBMITTED IN PARTIAL FULFILLMENT OF
THE REQUIREMENT FOR
THE DEGREE OF BACHELOR OF SCIENCE (INDUSTRIAL CHEMISTRY)
DEPARTMENT OF CHEMISTRY, FACULTY OF SCIENCE
KING MONGKUT'S INSTITUTE OF TECHNOLOGY LADKRABANG
ACADEMIC YEAR 2018

การพัฒนาวัสดุผสมระหว่างพอลิเมอร์และซีโอไลต์ เพื่อใช้งานเป็นตัวแยกน้ำในไบโอเอทานอล

THE DEVELOPMENT OF POLYMER-ZEOLITE COMPOSITE AS A MOLECULAR SIEVE FOR WATER REMOVAL IN BIO-ETHANOL

เขมรัฐ วรรณมหินทร์
อริยชัย มณีใส

โครงงานพิเศษนี้เป็นส่วนหนึ่งของการศึกษาตามหลักสูตร
ปริญญาวิทยาศาสตรบัณฑิต (เคมีอุตสาหกรรม)
ภาควิชาเคมี คณะวิทยาศาสตร์
สถาบันเทคโนโลยีพระจอมเกล้าเจ้าคุณทหารลาดกระบัง
ปีการศึกษา 2561

Title	The development of polymer-zeolite composite as a molecular sieve for water removal in bio-ethanol
Students	Mr. Khemmarat Wannamahintra Student ID 58050443
	Mr. Ariyachai Maneesai Student ID 58050574
Degree	Bachelor of Science (Industrial Chemistry)
Department	Chemistry
Faculty	Science
University	King Mongkut's Institute of Technology Ladkrabang (KMITL)
Academic Year	2018
Advisor	Dr. Kittisak Choojun
Co-advisor	Prof. Dr. Tawan Sooknoi

Faculty of Science, King Mongkut's Institute of Technology Ladkrabang (KMITL), has approved this special project submitted in partial fulfillment of the requirement for the degrees of Bachelor of Science (Industrial Chemistry) in academic year 2018.

Committees	Signatures
Assist. Prof. Dr. Panpailin Seeharaj Chairperson	Panpailin
Assoc. Prof. Dr. Patthavuth Monvisade Committee	
Dr. Kittisak Choojun Committee and Advisor	
Prof. Dr. Tawan Sooknoi Committee and Co-Advisor	

Title	The development of polymer-zeolite composite as a molecular sieve for water removal in bio-ethanol
Students	Mr. Khemmarat Wannamahintra Student ID 58050443
	Mr. Ariyachai Maneesai Student ID 58050574
Degree	Bachelor of Science (Industrial Chemistry)
Department	Chemistry
Faculty	Science
University	King Mongkut's Institute of Technology Ladkrabang (KMITL)
Academic Year	2018
Advisor	Dr. Kittisak Choojun
Co-advisor	Prof. Dr. Tawan Sooknoi

Abstract

This special project aims to develop polymer-zeolite composite as a pellet for water removal in bio-ethanol. The composite is compose of 95%wt of zeolite A and 5%wt of organic binder including poly(vinyl alcohol) (PVA) with three different grades (PVA JP-27, PVA GL-05, and PVA NL-05) and methyl cellulose (MC). The pellets were synthesized by extrusion method. The TGA results show that all types of PVA contains ~7%wt of water; while, MC contains ~2%wt of water. All these polymer binders started to decompose at 250 °C. The decomposition temperature of pellets is in the order of Z-PVAN < Z-PVAG < Z-PVAJ < Z-MC corresponding to molecular weight of polymers as a binder. According to the breakthrough curve at 80 °C after activation at 160-200 °C for 60 min, the %wt absorbed water (g/g) over each pellet is in the order of Z-MC < Z-PVAG < Z-PVAN < Z-PVAJ (7.79, 8.73, 9.14, 9.64%wt, respectively). Upon increasing the %water in ethanol solution (in other word decreasing the concentration of ethanol) zeolite-PVA JP-27 adsorbed all water resulting in 100% purity of EtOH prior the breakthrough point; while, the water capacity remains similar (~10%wt). As recyclability of zeolite-PVA JP-27 pellets for 5 times, the breakthrough curves resulted in almost the same characteristics.

Keywords: Adsorption, Zeolite A pellet, breakthrough curve, water removal, ethanol purification

หัวข้อโครงงานพิเศษ	การพัฒนาวัสดุผสมระหว่างพอลิเมอร์และซีโอไลต์ เพื่อใช้งานเป็นตัวแยกน้ำในไบโอเอทานอล	
ชื่อนักศึกษา	นายเขมรัฐ วรรณมหินทร์	รหัสนักศึกษา 58050443
	นายอริยชัย มณีโส	รหัสนักศึกษา 58050574
ปริญญา	วิทยาศาสตรบัณฑิต (เคมีอุตสาหกรรม)	
ภาควิชา	เคมี	
คณะ	วิทยาศาสตร์	
มหาวิทยาลัย	สถาบันเทคโนโลยีพระจอมเกล้าเจ้าคุณทหารลาดกระบัง (สจล.)	
ปีการศึกษา	2561	
อาจารย์ที่ปรึกษา	ดร.กิตติศักดิ์ ชูจันทร์	
อาจารย์ที่ปรึกษาร่วม	ศ.ดร.ตะวัน สุขน้อย	

บทคัดย่อ

โครงการพิเศษนี้มีวัตถุประสงค์เพื่อพัฒนาวัสดุผสมระหว่างพอลิเมอร์และซีโอไลต์ เพื่อใช้งานเป็นตัวแยกน้ำในไบโอเอทานอล โดยมีซีโอไลต์ A ปริมาณ 95%wt และพอลิเมอร์ที่ใช้เป็นตัวเชื่อม 5%wt ซึ่งตัวเชื่อมอินทรีย์ที่ใช้จะประกอบด้วย poly(vinyl alcohol) (PVA) 3 เกรด (PVA JP-27, PVA GL-05, PVA NL-05) และ methyl cellulose (MC) จากนั้นนำมา ขึ้นรูปแบบอัดรีดเม็ด ผลการวิเคราะห์การเปลี่ยนแปลง น้ำหนักของสารโดยอาศัยสมบัติทางความร้อน (TGA) พบว่า PVA ทุกชนิดประกอบด้วยน้ำ ~7%wt ในขณะที่ MC ประกอบด้วยน้ำ ~2%wt โดยที่พอลิเมอร์เหล่านี้จะเริ่มสลายตัวที่อุณหภูมิ 250 °C ในส่วนของเม็ดวัสดุผสม polymer-zeolite มีลำดับของอุณหภูมิในการสลายตัวเป็น Z-PVAN < Z-PVAG < Z-PVAJ < Z-MC ซึ่งเป็นผลมาจากน้ำหนักโมเลกุลของพอลิเมอร์ที่เป็นตัวเชื่อม จากกราฟของการดูดซับที่ 80 °C ภายหลังจากการกระตุ้นด้วยความร้อนที่ 160-200 °C เป็นเวลา 60 นาที ซึ่งปริมาณของน้ำที่สามารถดูดซับไว้บนวัสดุผสมคือ Z-MC < Z-PVAN < Z-PVAG < Z-PVAJ (7.79, 8.73, 9.14, 9.64%wt (g/g), ตามลำดับ) เมื่อทำการเพิ่มปริมาณของน้ำในสาละลายเอทานอล (หรือลดปริมาณ เอทานอล) ในกระบวนการดูดซับของ Z-PVA พบว่าน้ำถูกดูดซับไว้ได้ทั้งหมด ซึ่งให้เอทานอลบริสุทธ์ 100% สังเกตได้จากกราฟ ในขณะที่ปริมาณในการดูดซับยังคงเดิม (~10%wt) ความสามารถในการนำกลับมาใช้ใหม่ของวัสดุผสม zeolite-PVA JP-27 ที่ทำดูดซับต่อเนื่อง 5 ครั้ง พบว่ากราฟที่ได้ยังคงมีลักษณะคงเดิม

ACKNOWLEDGEMENTS

For the thesis completion, we would appreciatively thank our advisor, Dr. Kittisak Choojun for his supports, supervisions, inspiration, suggestions, advice and encouragements throughout this study for thesis. Also, we gratefully thank our Co-advisor, Prof. Dr. Tawan Sooknoi for his knowledge, advice, supports to teach and take care closely for this thesis as well as his kindness in every aspect. We also thank Assist. Prof. Dr. Panpailin Seeharaj and Assoc. Prof. Patthavuth Monvisade for serving on the committee and for their valuable comments and suggestions. We appreciate the supports from the Department of Chemistry, Faculty of Science, King Mongkut's Institute of Technology Ladkrabang, and also Catalytic Chemistry Research Unit (CCR) for the equipment, chemicals and facilities. We would like to extend our sincere appreciation to all teachers, industrial chemistry generation 34's friends, laboratory's staffs as well as the member of Catalytic Chemistry Research Unit for their constant guidance, advice, valuable supports and encouragement. Finally, we hope that this research will be beneficial and can be further developed. We appreciate and thank our family for their love and kindness.

Khemmarat Wannamahintra

Ariyachai Maneesai

CONTENT

CONTENT (Continued)

LIST OF TABLES

Table Page

Chapter 3

Chapter 4

Appendix A: GPC Results

Appendix C: GC-TCD Results

LIST OF TABLES (Continued)

Table Page

LIST OF FIGURES

Figure Page

Chapter 2

Chapter 3

Chapter 4

Appendix A: GPC Results

LIST OF FIGURES (Continued)

Figure Page

Appendix B: TGA Results

Appendix C: GC-TCD Results

LIST OF FIGURES (Continued)

Figure Page

CHAPTER 1

INTRODUCTION

1.1 Principle and rational

Ethanol (CH_3CH_2OH) is the most popular alcoholic bio-fuel at the present as an alternative to fossil fuels such as oil, coal and natural gases. Due to the depletion and the environment concern of these nonrenewable fossil fuels, the demand of ethanol has steady been steady growth. Ethanol can be produced from agricultural products known as bioethanol, which make it to be renewable energy source. However, the obtained ethanol that comes from distillation process, always contains at least 95.5% ethanol and 4.5% water [1]. These type of ethanol cannot be used in engine fuels. It has to be purified by dehydration process which is really hard and complicate to be able to use as engine fuels as it requires at least 99% ethanol. Thus, the bioethanol needs to be purified by dehydration process.

The refinery of ethanol can provide the 99.5% ethanol purity; however, it requires high energy and complicated to operate. The more efficiency purification and less complicate process is to use the absorbent.

Molecular sieve, such as Zeolite, can selectively absorb water due to the appropriate pore size and hydrophilic characteristics from their chemical properties. Commercially available zeolite has the range of pore size from 3 Å to 8 Å. Amongst these, Zeolite type 4A can effectively absorb water better than others [4]. Since the zeolite presents as a fine particle, it cannot be formed as pellet by its own. In order to form a pellet for the practical use, the binder is added to attach them together. In general binder can be classified as an inorganic and organic compounds.

Some of inorganic binders, such as Ball clay and kaolin have an ability to bind zeolite. Furthermore, they can convert their own structure to zeolite upon treatment by heat [6] because they compose of aluminosilicates, which are simple chemical composition of zeolite. However, the resulting composite brittle. As such, these inorganic binders have a limitation of use.

The organic binder is another compound that can bind zeolite forming a pellet. Polymers, such as polyvinyl alcohol (PVA) and methylcellulose (MC) had been reported to use as a binder which is easily formed a pellet by extrusion.

Furthermore, PVA and MC are considered as a hydrophilic polymer which could help the water adsorption [7]. Though, the temperature of use is limited by the decomposition of polymer (below 200 °C). As the grades of PVA depending on the molecular weight and hydrolysis, these could have an effect towards the water adsorption and temperature of use.

From all above reasons and principles, this project aims to study the use of different grades of polyvinyl alcohol (PVA) and methylcellulose (MC) forming zeolite pellet as a molecular sieve. The various commercial grades of PVA including JP-27, GL-05, and NL-05, were investigated. The stability of the obtained pellets was evaluated. The water adsorption ability by breakthrough characteristics and recyclability was studied using the manually design and built in fixed bed reactor equipped with Gas chromatography using thermal conductivity detector (GC-TCD).

1.2 Objectives

1.2.1 To develop Polymer-zeolite composite pellets by extrusion method.

1.2.2 To investigate the effect of types of commercial grade polymer binders in zeolite pellets.

1.2.3 To determine the water adsorption ability of zeolite pellets by using breakthrough curves

1.3 Scopes of this study

1.3.1 Make polymer-zeolite A pellets as a molecular sieve

1.3.2 Characterization of the polymer binder by Gel Permeated Chromatography (GPC) and zeolite pellets water adsorption capacity by Thermogravimetric analysis (TGA).

1.3.3 Adsorption rig design and built in.

1.3.4 Breakthrough Curves by Gas chromatography-Thermal Conductivity Detector (GC-TCD).

1.4 Expected results

1.4.1 Polymer-zeolite composite pellet would be made by extrusion method.

1.4.2 Obtained the effective Polymer-zeolite composite pellets for water removal in bio-ethanol.

1.4.3 Obtained breakthrough characteristics of each Polymer-zeolite composition which could be determined binders effect.

CHAPTER 2

THEORY AND LITERATURE REVIEW

2.1 Bioethanol

Bio-ethanol is a type of liquid fuel which can be produced from several biomass feedstock. Generally, the main feedstock for Bio-ethanol production is sugar crops, such as sugar cane, cassava, starch, and corn. There are several production processes which depend on the raw materials [1]. The common ethanol production carried out into the major three steps: i) to obtain the solution containing fermentable sugars, ii) conversion of sugars into ethanol by fermentation, and iii) the purification of ethanol. For the fermentation, the operation temperature is in between 25 °C and 30 °C and takes between 6 h and 72 h to finish depending on the composition of the hydrolysate, cell density, physiological activity and yeast species [ref]. Usually, the obtained ethanol purity is up to 95% ethanol. To further purify this solution, there are 3 main processes to purification ethanol 95% to absolute ethanol, the first process is azeotropic distillation made up to 99.6% alcohol purity [ref]. The higher purity of ethanol can be heteroazeotropic distillation using cyclohexane or benzene as an entrainers. However, it requires high energy and dangerous entrainer. Secondary, filtering (membranes technology) using pervaporation process by hydrophobic zeolite membrane, made up to 99.5% alcohol purity. The advantage is saving energy and nontoxic substances. Thus, membranes has a high cost. Third, adsorption process (molecular sieve) to remove excess water. Zeolite can separate ethanol 95.5% to 99.5% ethanol purity. This process is not complex and can be reused by regeneration.

2.2 Fermentation

Fermentation by-products Ethanol is produced by yeast fermentation. Although yeast mainly produces ethanol, it also produces by-products. These by-products need to be removed to obtain pure ethanol. There are mainly two kinds of by-product sources, starch and lignin. Starch derived by-products include esters, organic acids, and higher alcohols. Lignin derived by-products include cyclic and heterocyclic compounds.

2.3 Ethanol purification

Fermentation by-products are mostly removed by distillation. However, the trace volatile by-products remaining in ethanol causes the problems, especially for drinking and pharmaceutical purposes. Thus, the high purity of ethanol is required. There are several techniques to purify bioethanol including, distillation, rectification, and adsorption, for example.

2.3.1) Distillation

Distillation is the most dominant and recognized industrial purification technique of ethanol. It utilizes the differences of volatilities of components in a mixture. The basic principle is that upon the heating a mixture, low boiling point components are concentrated in the vapor phase. By condensing this vapor, more concentrated less volatile compounds is obtained in liquid phase. Thus, distillation is one of the most efficient separation techniques. However, it contains several problems. One is separation of relatively close boiling point volatile compounds. In ethanol production, a distillation tower is designed to separate water and ethanol effectively. Water is obtained from the bottom of the tower and ethanol is obtained from the top of the tower. It is expected that impurities with similar boiling points to ethanol lodges in ethanol even after distillation. Second is its cost. Distillation is a repetition of vaporization and condensation. Therefore, it costs a lot.

2.3.2) Rectification

Rectification is an application of distillation and its uses include fractionation of crude oil. If the distillate obtained during distillation is distilled again, the new distillate would contain higher concentration of volatile components. As the procedure is repeated, the concentration of volatile components in the distillate increases on each occasion. In practice, this multi-stage distillation process is carried out in the form of countercurrent distillation (rectification) in a column. The liquid mixture to be separated (feed) is fed to the bottom of the column, where it is brought to boiling point. The vapor produced moves upwards inside the column, and

then is condensed. Part of the condensation is carried away as top product. The remainder flows back into the column and moves downwards as liquid opposite phase.

2.3.3) Adsorption

Adsorption is a separation technique utilizing a large surface area of absorbent. Compounds are simply absorbed on the absorbent depending on their physical and chemical properties. In general, bigger particles tend to be absorbed more due to their low diffusivities. Also, compounds with the similar polarity to the absorbent surface tend to be absorbed more. When purification of ethanol is considered, non-polar surface and wide ranging pore distribution are favorable since ethanol is polar compounds and various sizes of particles could be contained in ethanol as impurities. From water treatment, activated carbon (Demirbas et al., 2008) and activated alumina (Tripathy and Raichur, 2008) are the most expectable absorbents.

2.4 Zeolite A

Zeolite is a hydrated of aluminocilicate having tetrahedral structure. It consists of silicon atom or aluminium atom bonded with 4 of oxygen atoms (SiO_4 or AlO_4) on the framework called the primary building units. Because of the negative framework charge from aluminium that is in tetrahedral structure, the charge balancing by cations, such as sodium, potassium and calcium, is typically present. There are several types of zeolites as shown in Figure 2.1. In addition, the structure could also contain water in the zeolite crystal void. With all these elements, zeolite has many features, such as adsorption, ion exchange and catalysis.

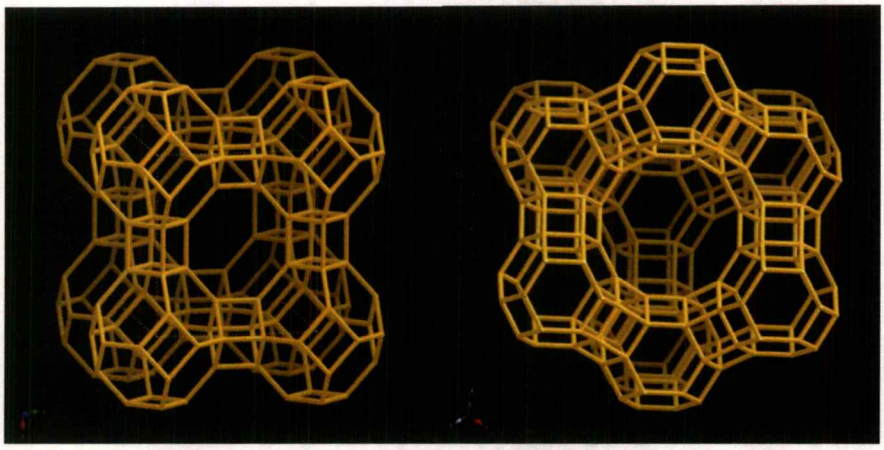

Zeolite LTA Zeolite FAU

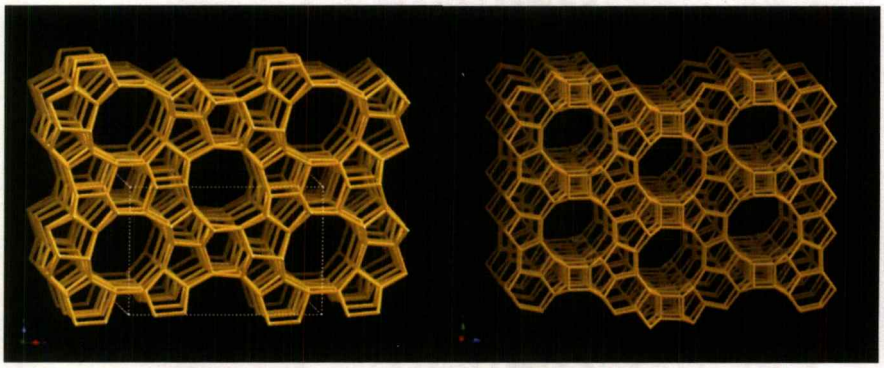

Zeolite MFI Zeolite BEA

Figure 2.1 Types of zeolites

Zeolite A is an aluminosilicate compound with the Si/Al ratio about 1 as shown in Figure 2.2. Thus, zeolite A has a high polarity which can absorb water well called hydrophilic structure. Furthermore, it can absorb the desired molecules which is smaller than its porous size. This creates the selective adsorption in which the smaller molecules can pass through; while, large molecules cannot get inside the pores. As such, the molecules fitting in the porous of zeolite are trapped within the framework.

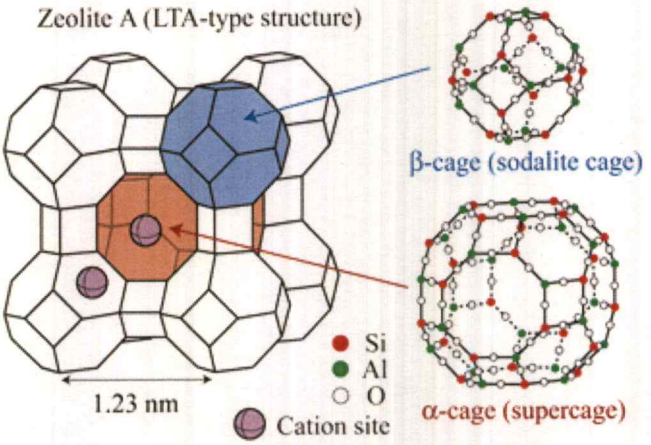

(image from http://www.sssj.org/ejssnt/duan-small.jpg)

Figure 2.2 Structure of zeolite A

Normally, Zeolite A cannot be formed as pellets. It is necessary to use a binder to make the zeolite A as a pellet.

2.5 Binder

Binders are loosely classified as organic (bitums, animal and plant glues, polymers) and inorganic (lime, cement, gypsum, liquid glass, etc.). These can either be metallic or ceramic as well as polymeric depending on the nature of the main material. For example, in the compound WC-Co (Tungsten Carbide used in cutting tools) Co constitutes the binding agent for the WC particles

2.5.1 Inorganic binder

Inorganic binders are inorganic substances which are usually produced by heat treatment of natural raw materials of suitable composition. Inorganic binders are agents (mixture of substances), which have the ability of self-hardening, thus connecting granular systems in a rigid compact whole. Into the whole, binders can also accommodate a filler as a composite material. Mixing inorganic binder with the desired quantity of water results in a well workable mass, which subsequently solidifies and hardens.

2.5.2 Organic binder

An organic binder is an organic ingredient used to bind together two or more other materials in mixtures. Its two principal properties which are adhesion and cohesion makes organic binder practical to use.

2.5.1.1 Polyvinyl alcohol (PVA)

Polyvinyl alcohol has the chemical formula of $[CH_2CH(OH)]_n$. They has melting point around 200 °C. Furthermore, it is soluble in water. PVA is a synthetic polymer that is non-toxic and odorless. PVA can be formed as a film which has the property as an adhesion (glue), flexible, good tensile strength and good resistance to permeability of oxygen. However, water permeability is low because the molecule has polarity when put in high relative humidity conditions, it can cause swelling. PVA can also be biologically decomposed [10].

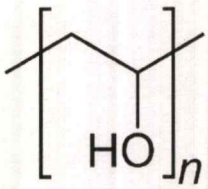

Figure 2.3 Molecular structure of polyvinyl alcohol (PVA)

2.5.1.2 Methyl cellulose (MC)

Methyl cellulose (MC) has the chemical formula of $C_6H_7O_2(OH)_x(OCH_3)_y$. It is obtained from cellulose which is extracted from reacting wood or cotton wool with alkali and methyl chloride, respectively. MC is a white crystalline powder which is soluble in cold water forming a clear viscous solution or gel. However, it do not dissolve in hot water. MC is used in many industries, such as fillers in natural gums, glue, and adhesives to increase strength, flexibility, and adhesion strength [11].

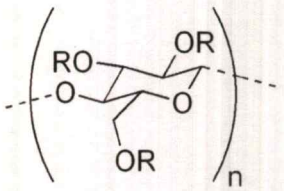

R = H or CH_3

Figure 2.4 Molecular structure of methyl cellulose (MC)

2.6 Mass transfer zone

Mass transfer zone is a zone where adsorption occurs in fixed bed. The concentration of the solution that move through the bed will come out as 0 and increase overtime to saturate. Ratio of outlet solute concentration to inlet solute concentration in the fluid as a function of time from the start of flow. The S-shaped curve is called the breakthrough curve.

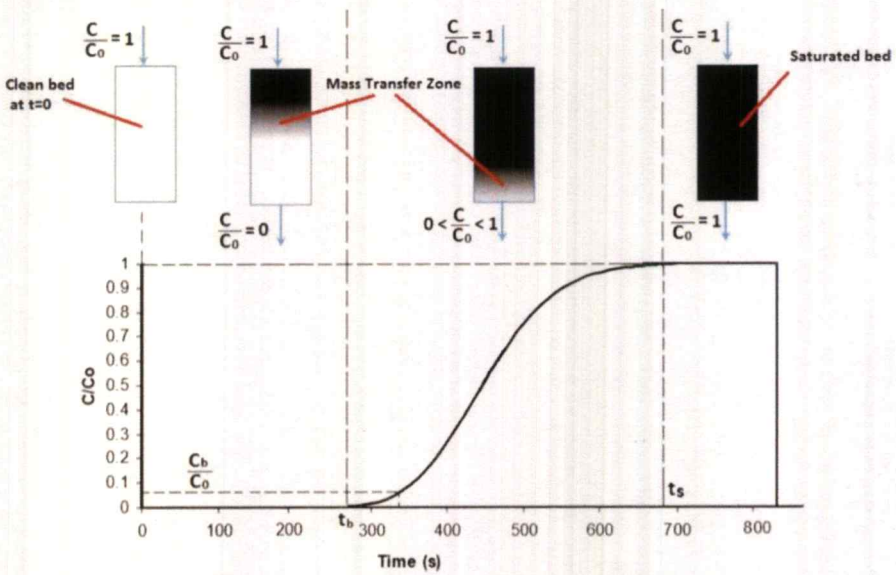

Figure 2.5 Mass transfer zone with breakthrough curve

The time which the ratio of C/C_0 begin to increase is called breakthrough point, this point can be considered as true capacity of fixed bed. The solution that came out after the breakthrough point are not preferred because of the dropping in purity. In industrial usage of fixed bed the adsorption process only perform until near breakthrough point to prevent the impurity of products.

2.7 Literature review

Ethanol is the most popular alcoholic biofuels at the present world market. It is produced from renewable agricultural resources, such as corn, sugar and molasses. Furthermore its less toxic than other alcoholic fuels, and its by-products formed in the process are almost non-toxic, have drawn much attention. Mustafa, V., *et al.* (2013) reported that ethanol production could be carried out into major three steps: (1) to obtain the solution containing fermentable sugars, (2) conversion of sugar into ethanol by fermentation and (3) ethanol separation and purification in which this steps usually use distillation-rectification-dehydration. Ethanol from distillation process is commonly made up of 95.5% alcohol and 4.5% water that known as "hydrous" or "hydrated" ethanol. It is then dehydrated to obtain "anhydrous" ethanol containing up to 99.6% alcohol and 0.4% water that will be used as fuel [1].

The usage of molecular sieve, solid with very narrow and uniform porosity, is one of the several methods to separate the mixture of ethanol and water. Alcaniz-Monge, J., *et al.* (2002) showed that the size of molecular sieve (CMS) are almost non-significant to water from 95.5% ethanol solution [2]. Another type of molecular sieve is Zeolite. Laetitia, B., *et al.* (2015) suggests that zeolite material have been recognized as promising candidates for multifunctional applications, such as catalysis, ion-exchange, gas separation, etc. In addition, zeolite materials are also of scientific and technological importance because of their ability to absorb and inter act with atom and molecules [3].

There are numerous naturally occurring and synthetic zeolites. Sowerby, B., *et al.* (1988) reported that the zeolite type 4A has better water absorption ability than others. Though these materials cannot be formed as pellets. They require another material to attach them together which is called binder. In general, binder can be classified as an organic and inorganic compounds [4].

Mousa, G., *et al.* (2014) reported that inorganic binders, such as Ball clay and Kaolin have ability to bind zeolite, but these binders make pellets hard but brittle characteristics [6]. The organic binder is another alternative compound, especially a polymer. Chaiwat, R., *et al.* (2007) reported that polyvinyl alcohol (PVA) or methylcellulose (MC) mixed with zeolites are easily to extrude and their stability are good in the usage at low temperature [7].

The extrusion method are good for making pellets with high density and mechanical strength. This method is the most commonly applied shaping technique for catalysts or catalyst supports. Many types of extrusion equipment are used, some of which are very sophisticated, but the process is in principle very simple.

To measure the adsorption ability of these zeolite pellets, the breakthrough curve of adsorption of water in the pellet is necessary. Jens, W., *et al.* (1991) reported the method to obtain the breakthrough curve of gas phase adsorption. By using NaX and NaY as hydrophobic absorbent in separation of gaseous water/ethanol mixtures [8]. By using Zeolite A as absorbent Marian, S., et al. (2009) reported the adsorption/desorption of water and ethanol on 3A Zeolite in near adiabatic Fixed bed in the form of a mathematical model for bench scale adsorption bed included the linear driving force (LDF) adsorption rate model and the variation of axial velocity. A detailed heat transfer model to analyze the experimental data and extract values of pertaining diffusion coefficients [9].

CHAPTER 3

Research Methodology

3.1 Reagents

	Chemicals	Grade of purity	Manufacturers
1.	Zeolite A	-	PQ CHEMICALS
2.	Poly(vinyl alcohol) (PVA)	JP-27	-
3.	Poly(vinyl alcohol) (PVA)	GL-05	-
4.	Poly(vinyl alcohol) (PVA)	NL-05	-
5.	Methylcellulose (MC)	-	GAMMACO
6.	Sodium chloride (NaCl)	Analysis	LOBA CHEMIE
7.	Absolute ethanol	-	SIGMA-ALDRICH
8.	Isopropanol	-	-
9.	DI water		-

3.2 Apparatus

1. Laboratory glassware, plastic ware
2. Syringe pump and plastic syringe
3. Oven
4. Hot plate and stirrer
5. Thermal gravimetric analyzer (TGA), Perkin Pyris1 TGA
6. Gas Chromatography –Thermal Conductivity Detector (GC-TCD)

3.3 Preparation and Characterization of pellets.

3.3.1 Pellets synthesis

(1) PVA-Zeolite A pellet

0.27 g of PVA (The grade are GL-05, JP-27 and NL-05) was first dissolved in 4 mL of DI H_2O. Then, this solution was mixed with 5.00 g of zeolite A. After that, this mixture was rested for 3 h. The resulting mixture was then extruded by syringe pump at speed of 89 mL/h. The extruded mixture was dried at 150 °C overnight and cut to the length of 2 mm with 1.6 mm diameter.

(2) MC-Zeolite A pellet

The preparation is similar to PVA-Zeolite pellet but using MC instead of PVA.

3.3.2 Characterization

3.3.2.1 Thermogravimetric analysis (TGA)

Thermogravimetric analysis or Thermogravimetric analysis (TGA) is a method of thermal analysis in which the mass of a sample is measured over time as the temperature changes. This measurement provides information about physical phenomena, such as phase transitions, absorption, and desorption; as well as chemical phenomena including chemisorptions, thermal decomposition, and solid-gas reactions

Zeolite pellets were kept on watch glass in seal container that contain saturated sodium chloride solution for at least 24 h to absorbed moisture. Then, the water composition of zeolite pellet and their stability were studied by Thermogravimetric analysis (TGA).

3.4 Determination of the adsorption ability of Polymer-zeolite composite pellets

The adsorption ability of Polymer-zeolite pellets was determined by breakthrough curves which can be obtained from the in-house building rig equipped with Gas chromatography using Thermal conductivity detector (GC-TCD) as shown in Figure 3.1.

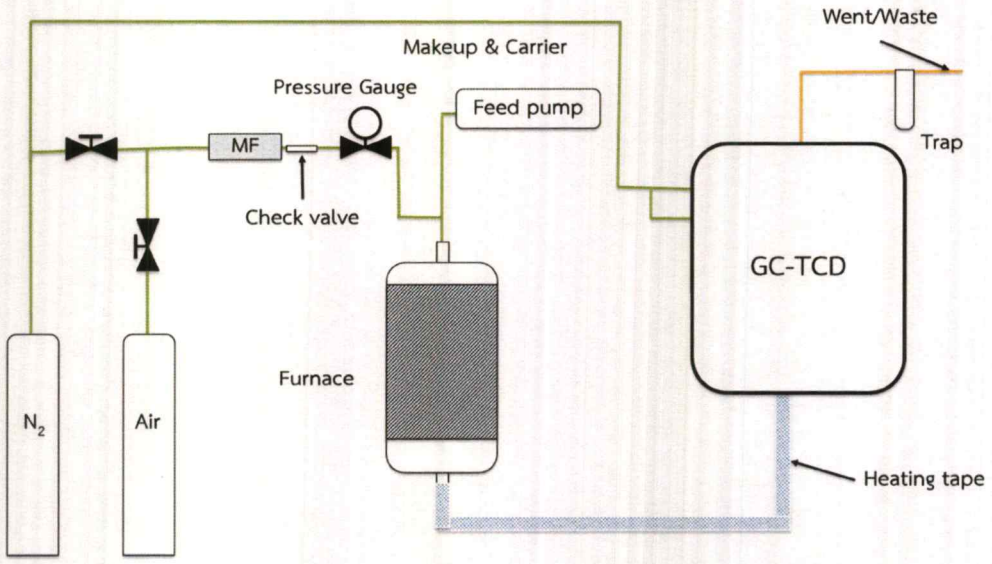

Figure 3.1 Adsorption rig schematic design

3.4.1 Activation

1g of Polymer-zeolite pellets was packed in glass tube for 8cm which is in the desired heating zone (5 cm above and 3 cm below the center for tube furnace). After setting up, the pellets were activated at 200 °C under air with the flow rate of 20 mL/min. Noted that the furnace was set at 210 °C which resulted in the temperature of packing zone in 164-205 °C.

3.4.2 Adsorption

After the activation, the air was switched to nitrogen at the flow rate of 20 mL/L in order to flush the system including the line of loading six-port valve. The system was flushed at least 30 min. To make sure that there is no water in the system, the injection of GC-TPD was performed prior introduced ethanol to double check the trace amount of water. After that, the solution of certain purity of ethanol (85, 90, 95%) was introduced with feed rate of 2 mL/h. The amount of water and ethanol after adsorption at certain time was determined by GC-TCD with the condition as shown in table 3.2.

Table 3.1 GC condition for the determination of water and ethanol

Parameter	Set Value
Inlet	Inj. Temp. : 200° C
	Split ratio : 50:1
Column	PlotQ 25.0 m x 320 μm x 10 μm
	Constant flow 2.0 ml/min
Oven	Oven Temp. : 180° C (hold 6 min)
Carrier gas	N_2 high purity ,Constant flow
	Linear velocity : 33 cm/sec @ 180 ° C
Detector	TCD @ 170° C

3.2.1 Desorption

Desorption of pellets after the adsorption was similar to the activation condition in which desorption time were varied from 30, 60 to 90 min.

3.5 Calculation of water percentage in polymer zeolite composite pellet

The water percentage in pellets could be determine by using following equation.

$$\frac{\%water\ in\ EtOH\ solution\ \left(\frac{g}{g}\right) x\ EtOH\ feed\ density\ \left(\frac{g}{mL}\right) x\ Feed\ rate\ \left(\frac{mL}{h}\right) x\ Breakthrough\ point\ (h)}{Composite\ pellets\ weight\ in\ fixed\ bed\ (g)}\ x\ 100$$

Equation for water percentage in pellets calculation

CHAPTER 4

RESULT AND DISCUSSION

4.1 Polymer characterization

The molecular weight of the commercial poly(vinyl alcohol) (PVA) grade GL-05, JP-27, NL-05, and methylcellulose (MC) as first determined by Gel permeation chromatography (GPC) (seen in Appendix A). The result is summarized in **Table 4.1.**

Table 4.1 Molecular weight of polymers determining from GPC

Type of polymer	$\bar{M}_w$ (Dalton)	$\bar{M}_w/\bar{M}_n$ (PDI)	Intrinsic Viscosity*	Degree of hydrolysis (%)*
PVA JP-27	-	-	50 - 60	87 – 89
PVA GL-05	13,475	2.35	4.8 - 5.8	86.5 - 89
PVA NL-05	21,024	1.95	4.6 - 6.0	98.5
MC	1,067,012	6.55	-	-

***From various supplier label**

As seen in **Table 4.1**, the molecular weight of PVA is in the order of NL-05 < GL-05 < JP-27. The similar trend is also observed for the intrinsic viscosity. Polydispersity index (PDI) in all PVA polymers quite low. This indicates the similar molecular weight distribution of PVA. All of the PVAs are considered as a high degree of hydrolysis. Methyl cellulose (MC) has the highest molecular weight and its PDI is relatively high as compared to those of PVA polymers. This suggests that the distribution of MC molecular weight is considered in large range.

The Thermogravimetric analysis (TGA) of each polymer is shown in **Figure 4.1.**

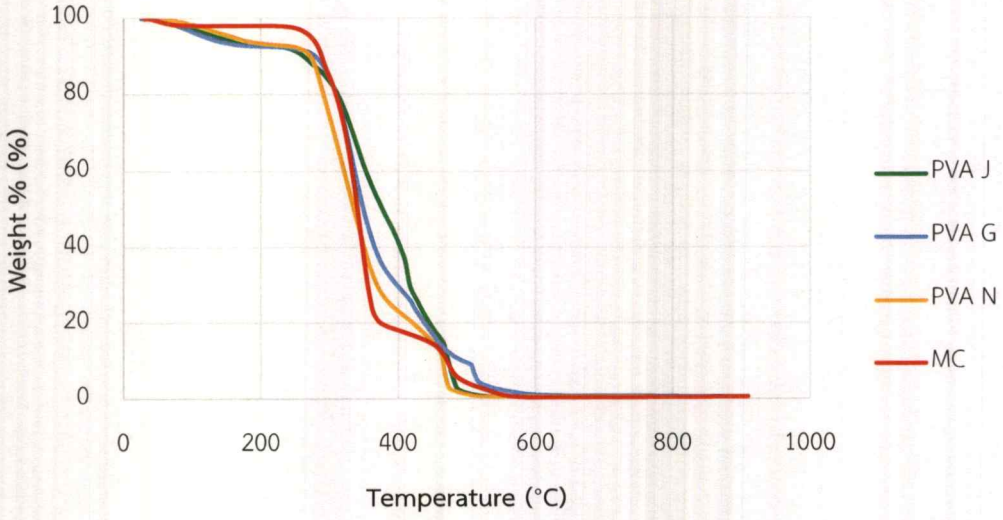

Figure 4.1 TGA Profile of polymers

It can see in **Figure 4.1** that all polymers have two main weight losses. The first one could attribute to the mass loss of absorbed water at 30-200 °C. For the second one, it corresponds to the mass loss of polymer decomposition at 250-600 °C. All polymers are completely decomposed at 600 °C. Once considering the amount of absorbed water in these polymers, all PVA grades have quite similar amount of water content (7.08%wt, 7.23%wt, 7.00%wt for PVA JP-27, PVA GL-05, PVA NL-05, respectively), regardless to those different hydrolysis. While, MC absorbs lower water (1.9%wt) indicating the lower hydrophilic properties. The decomposition temperature of polymers increases from PVA NL-05 < PVA GL-05 < PVA JP-27 < MC (250 °C, 255 °C, 260 °C, 280 °C, respectively), which could be the result of their molecular weight. Noted that, the decomposition of all polymers begins at 250 °C. This limits their use at temperature above 250 °C.

4.2 Pellet composition and characterization

The mixture of 95%wt of zeolite A and 5%wt of polymer in 4 mL of water was extruded to form pellets via the syringe pump. The list of pellet composition is shown in **Table 4.2.**

Table 4.2 Composition of pellets

Pellet	Zeolite A (g)	PVA JP-27 (g)	PVA GL-05 (g)	PVA NL-05 (g)	MC (g)
Z-PVAJ	5.0	0.27	-	-	-
Z-PVAG	5.0	-	0.27	-	-
Z-PVAN	5.0	-	-	0.27	-
Z-MC	5.0	-	-	-	0.27

The thermal stability of all pellets were investigated by the Thermogravimetric analysis (TGA). Prior running the TGA, all pellets were kept at 75% humidity using saturated sodium chloride overnight. The results are shown in **Figure 4.2.**

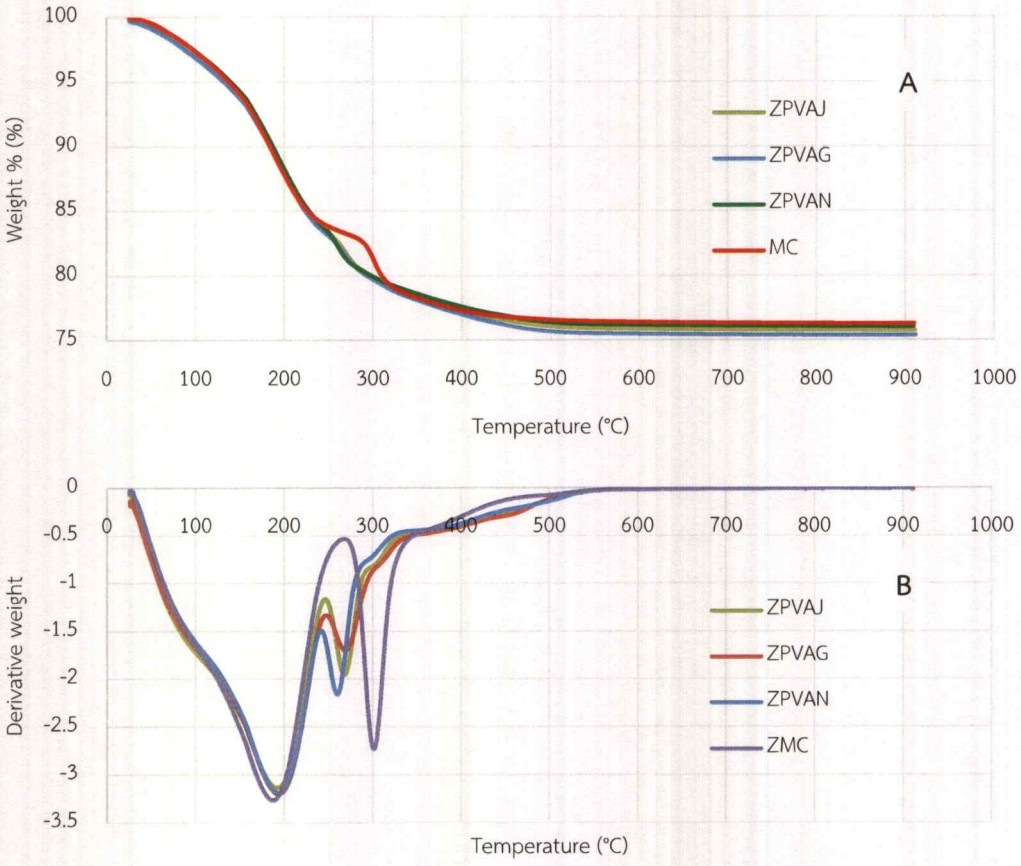

Figure 4.2 TGA Profile in pellets

According to **Figure 4.2**, all pellets show two main weight losses at 30-200 °C and 250-500 °C. This corresponds to the absorbed water and polymer decomposition, respectively. The absorbed water in all pellets is ~16%wt as shown in **Table 4.3** regardless to the types of polymers. All pellets containing around ~6%wt of polymer (subtracting the absorbed water, **Table 4.3**) and the remaining weight at ~75% could attribute to the zeolite which cannot decompose at this range of temperature. The decomposition temperature of pellets is in the order of Z-PVAJ < Z-PVAG < Z-PVAN. This difference in decomposition temperature could attribute to molecular weight of polymers as a binder. For Z-MC, it has the highest decomposition temperature due to the highest molecular weight of MC.

Table 4.3 Water percentage of each pellet composition determining from TGA

Pellets	%wt water	%wt polymer
Z-PVAJ	16.39	6.38
Z-PVAG	16.43	6.55
Z-PVAN	15.92	6.57
Z-MC	16.57	5.80

4.3 Breakthrough Curve

4.3.1 System setup

The calibration curve of water in ethanol solution was first determined by the Gas chromatography equipped with thermal conductivity detector (GC-TCD). The calibration curve is shown in **Figure 4.3.**

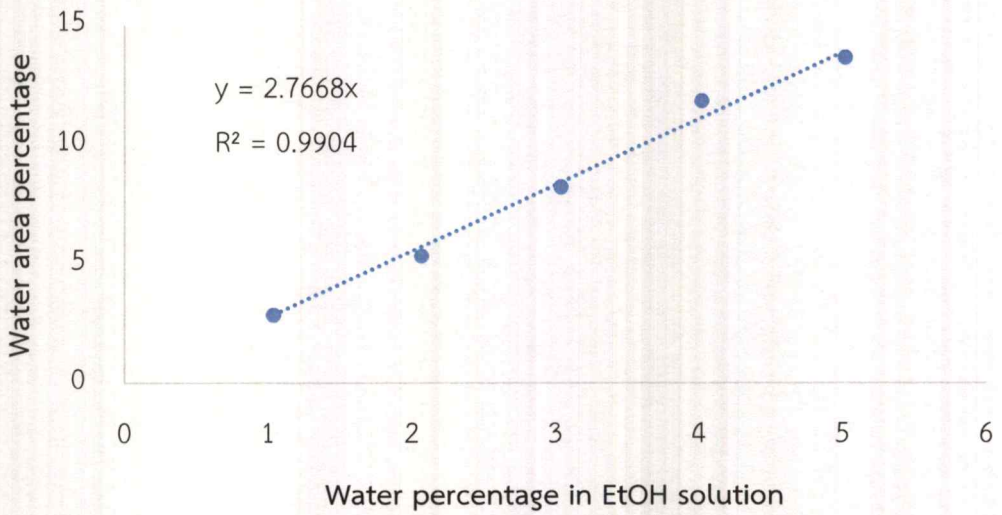

Figure 4.3 Calibration of water percentage in ethanol solution with water area percentage

It can be seen in **Figure 4.3** that calibration curve is linear with R^2 of 0.99. This will be used to determine water concentration in ethanol solution.

As the breakthrough curve was tested in the continuous gas flow fixed bed reactor, the system was thus validated by determining the %water in ethanol (including 95%, 96%, 97%, 98%, and 99%wt) using this setup compared with the manual injection The concentration detected by GC-TCD is shown in **Table 4.4.**

Table 4.4 Comparison of ethanol solution concentration from each method

Prepared ethanol solution concentration (%wt)	Manual injection method concentration (%wt)	Feed injection method concentration (%wt)	Δ Detection
99	98.96	98.98	0.02
98	97.93	97.95	0.02
97	96.96	96.83	0.13
96	95.98	95.89	0.09
95	94.98	94.79	0.20

As can be seen in **Table 4.4,** the concentration of direct injection method and feed injection method (continuous gas flow) are almost the same. This clearly indicates that the system is operational.

4.3.2 Optimization of bed length

The effect of bed length towards the breakthrough curve using Z-PVAJ was determined by packing at 5 cm and at 8 cm in 8 mm diameter glass tube using 95%wt ethanol as a feed. The result is shown in **Figure 4.4.**

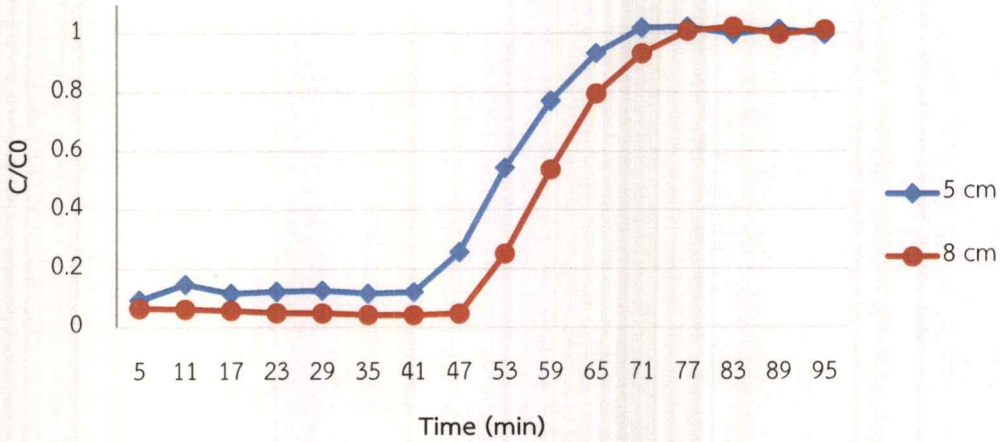

Figure 4.4 Effect of bed length to breakthrough curve

From **Figure 4.4,** the initial amount of water that came out from fixed bed, packing for 5 cm bed length is higher than that of 8 cm. Ideally, with the different in bed length, the only capacity should be different. However, in this case the difference in initial solution concentration was observed (~99.88% and ~99.95% in purity of EtOH for 5 cm and 8 cm, respectively). This indicates that the bed length of 5 cm is too short resulting in the through bed. This means that when the solution flow through the bed, it cannot absorb all water in the solution. As such, some of the water molecules flow through the bed with ethanol without adsorption causing the lower purity of EtOH. Even though, using the bed length of 8 cm in this system can absorb more water, the through the bed was still observed. To eliminate this problem, the carrier gas flow rate was further optimized.

4.3.3 Optimization of carrier gas flow rate

The effect of carrier gas (N_2) flow rate at 10 mL/min and 20 mL/min towards the breakthrough curve using Z-PVAJ was determined using 95%wt ethanol as a feed. The result is shown in **Figure 4.5.**

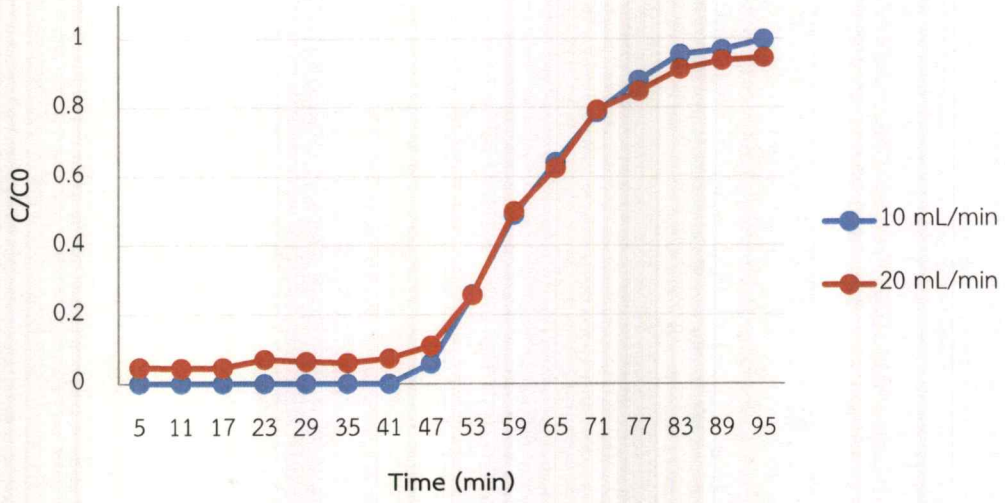

Figure 4.5 Effect of carrier gas flow rate to breakthrough curve in Z-PVAJ pellet

From the breakthrough curve in **Figure 4.5**, the breakthrough point of both flow rate is at 41 min. 10 mL/min flow rate gives 100%wt ethanol; while, 20 mL/min flow rate gives 99.6%wt ethanol purity. This indicates that the through bed is eliminated in 10 mL/min flow rate providing 100% purity of ethanol. In summary, the use of carrier gas flow rate set to 10 mL/min and bed length of 8 cm is the optimization.

4.3.4 Optimization of desorption time

The effect of desorption time towards the breakthrough curve using Z-PVAJ was determined using 95%wt ethanol as a feed with the carrier gas (N_2) flow rate of 10 mL/min. The effect of desorption time at 30, 60, and 90 min were determined. The result is depicted in **Figure 4.6.**

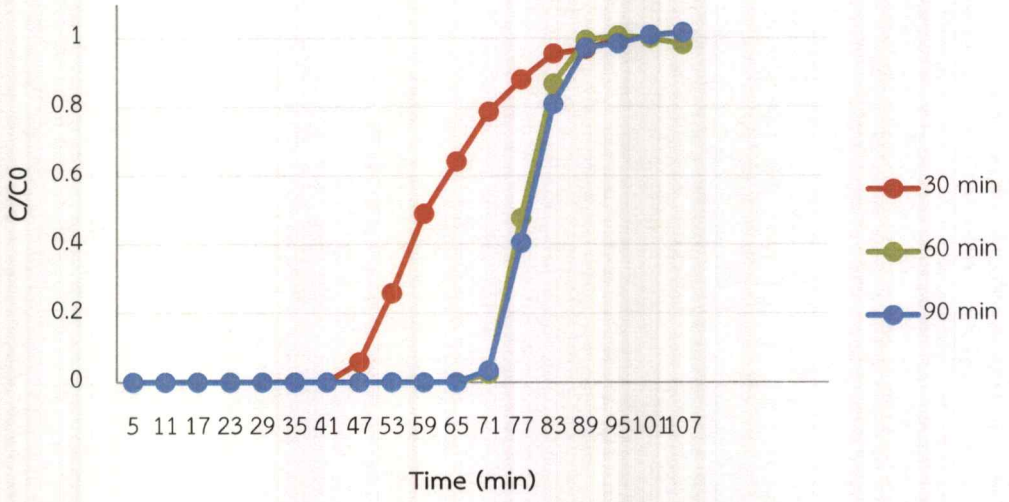

Figure 4.6 Effect of desorption time to breakthrough curve in Z-PVAJ pellet

As seen in **Figure 4.6,** all desorption times at 30, 60, and 90 min give 100%wt ethanol. However, the desorption time at 30 min shows the lower breakthrough point (41 min) as compared with those two (65 min). This indicates that the capacity of 30 min desorption is lower than others. Furthermore, the slope of the breakthrough curve in 30 min desorption is less than that of 60 and 90 min desorption. This indicates the lower strong interaction of Z-PVAJ and water at the desorption time of 30 min. This could attribute to remaining water in the Z-PVAJ causing both lower in capacity and adsorption strength. Since the desorption time of 60 and 90 min gave almost exactly same breakthrough curve, the desorption time at 60 min was thus selected for further studies.

4.3.5 Effect of Binder

The breakthrough curve of Z-PVAN, Z-PVAG, Z-PVAJ, and Z-MC pellets was examined by using 1 g of each pellet packing 8cm of bed length with the N_2 carrier gas flow rate of 10 mL/min and 95% ethanol concentration. The result is shown in **Figure 4.7.**

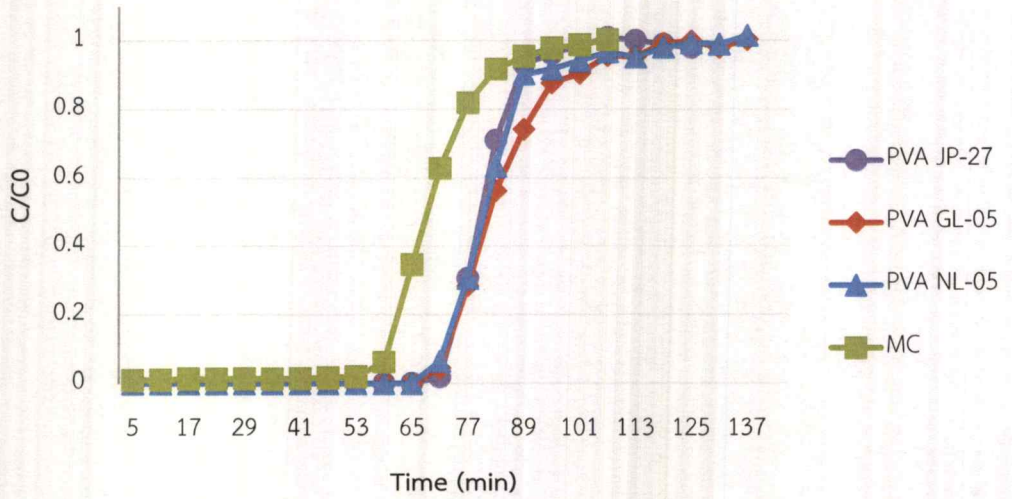

Figure 4.7 Effect of polymer binder to breakthrough curve of various pellets

It can be seen that the breakthrough point of Z-MC is at 53 min and the others are at ~65 min. The capacity determining from the breakthrough point is summarized in **Table 4.5.** The %wt absorbed water (g/g) over each pellet is in the order of Z-MC < Z-PVAN < Z-PVAG < Z-PVAJ (7.79, 8.73, 9.14, 9.64, respectively). As expected, the Z-MC has the lowest capacity as observed in TGA. This could attribute to the lowest hydrophilic property as compared with others. In supporting manner, the steepness of slope is in order of Z-MC < Z-PVAG < Z-PVAN ~ Z-PVAJ. This thus emphasizes the lowest adsorption strength of MC binder. In addition, the PVA polymers have been hydrolyzed resulting the hydroxyl group. This could enhance their adsorption capacity as compared to MC. For PVA polymers, the PVA JP-27 grade as a binder has the highest capacity. This could be the result of the highest intrinsic viscosity and highest molecular weight of this polymer compared with others causing the lower dispersed once mixing with zeolite A. As such, the exposed surface and

pore site of the composite could be more. While, the other two PVA binders are of similar as their properties. Noted that all pellets provide 100% EtOH purity.

Table 4.5 Water percentage in each composition pellets

Composition	Breakthrough point (min)	%wt water
Z-PVAJ	70.91	9.64
Z-PVAG	70.66	9.14
Z-PVAN	71.38	8.73
Z-MC	58.41	7.79

4.3.6 Effect of concentration

As Z-PVAJ pellets having the best breakthrough curve characteristics, they was thus selected to evaluate the adsorption ability upon various the concentration of ethanol solution from 85-95%wt. The results are demonstrated in Figure 4.8.

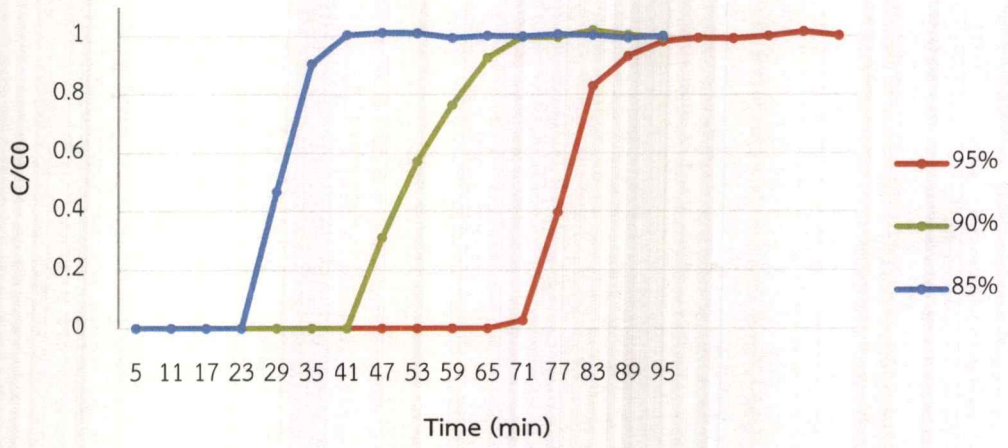

Figure 4.8 Effect of ethanol concentration to breakthrough curve in Z-PVAJ

As can be seen from **Figure 4.8,** the breakthrough point is 23, 41, and 65 min for 85, 90, 95%wt EtOH concentration. All water was adsorbed by Z-PVAJ resulting in 100% purity of EtOH prior the breakthrough point. Furthermore, even with high amount of water in feed solution, the characteristics of breakthrough curve are still almost the same. This suggests that this pellet can be applied in high water-ethanol mixture.

Table 4.6 Water percentage in Zeolite-PVA JP-27 pellets with different feed concentration

Ethanol feed concentration (%wt)	Breakthrough point (min)	%wt water
95	71.18	8.87
90	48.52	11.54
85	24.68	9.42

4.3.7 Recyclability

The recyclability of Z-PVAJ pellets was tested using 95% EtOH as a feed. The results is shown in **Figure 4.9** and the water adsorption capacity is summarized in **Table 4.7.**

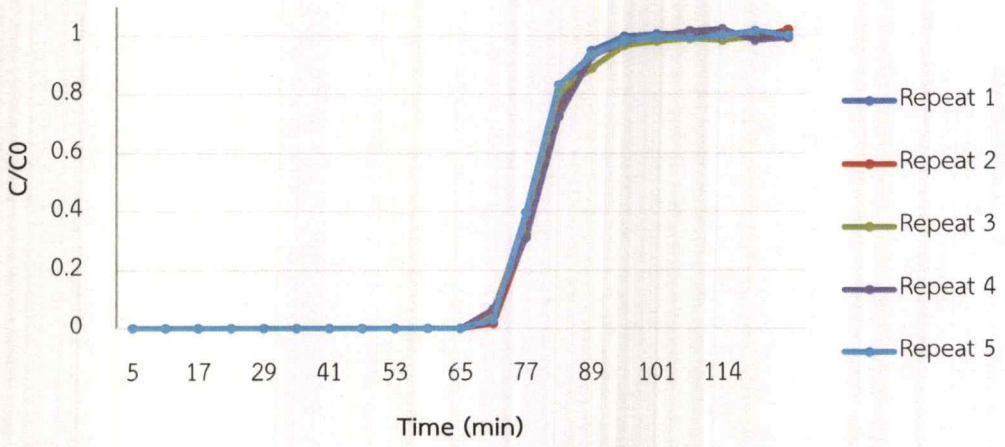

Figure 4.9 Breakthrough curve of each repeat in Z-PVAJ usage

Table 4.7 Water percentage in Zeolite-PVA JP-27 pellets with repeat experiments cycle

Adsorption and desorption cycle	Breakthrough point (min)	%wt water
Repeat 1	70.17	9.98
Repeat 2	70.75	9.70
Repeat 3	70.05	9.78
Repeat 4	71.23	9.54
Repeat 5	70.09	9.67

According to **Figure 4.9,** the breakthrough characteristics of Z-PVAJ pellets remain the same with 5 repeating adsorption sequence. Furthermore, their adsorption capacity as summarized in **Table 4.7** is the same. This result suggests that Z-PVAJ does not degrade at this range of temperature of use. Thus, it can be applied for water separation to purify ethanol for several times.

CHAPTER 5

CONCLUSION AND SUGGESTIONS

5.1 Conclusions

This special project study the development of polymer-zeolite composite pellets as a molecular sieve for water removal in bio-ethanol. The composites compose of 95%wt of zeolite A and 5%wt of organic binder including poly(vinyl alcohol) (PVA) JP-27, PVA GL-05, PVA NL-05, and methyl cellulose (MC). In the preparation, the mixture of zeolite A and a polymer was extruded by syringe pump at speed of 89 mL/h. The extruded mixture was dried overnight and cut as a pellet.

The results of thermos gravimetric analysis (TGA) profiles show that all type of PVA contains water in their structure (~7%wt); while, MC has the lower absorbed water (~2%wt). All these polymer binders decomposed at 250 °C, which is the limitation temperature for removing water and regeneration of pellets. The decomposition temperature of pellets is in the order of Z-PVAN < Z-PVAG < Z-PVAJ < Z-MC. This difference in decomposition temperature could attribute to molecular weight of polymers as a binder.

According to the breakthrough curve at temperature for adsorption is 80 °C, the %wt absorbed water (g/g) over each pellet is in the order of Z-MC < Z-PVAN < Z-PVAG < Z-PVAJ (7.79, 8.73, 9.14, 9.64%wt, respectively). Noted that all pellets provide 100% EtOH purity. In term of both thermal stability and water adsorption capacity, Z-PVAJ pellet has the best performance. This could attribute to both the high molecular weight and high hydrophilic property (high %hydrolysis).

Upon increasing the %water in ethanol solution (in other word decreasing the concentration of ethanol), all water was adsorbed by Z-PVAJ resulting in 100% purity of EtOH prior the breakthrough point while the water capacity remains similar. The recyclability of zeolite-PVA JP-27 pellets for 5 times, the breakthrough curves result in almost the same characteristics.

5.2 Suggestions

5.2.1 This work only used two type of organic binder. In the next study, used more type of organic binder with high molecular weight and degree of hydrolysis for the most efficiency in water adsorption with the same amount of pellets.

5.2.2 This work only experiment on 5 repeat of the most effective type of pellet cause of limited study time. In the next study, repeat the adsorption sequence of pellet as much as the time allowed. For the most efficiency in industrial usage.

REFERENCES

1. M. Vohra, J. Manwar, R. Manmode, S. Padgilwar, S. Patil "Bioethanol production : Feedstock and current technologies" Journal of Environmental Chemical Engineering 2 (2014) 573–584
2. J. Alcaniz-Monge, D. Lozano-Castello "Assessment of ultramicroporosity on carbon molecular sieves by water" Studies in Surface Science and Catalysis 144 (2002) 201-208.
3. B. Laetitia, T. Jean Doau, A. Simon Masseron, C. Gerald, P. Joel "Synthesis of EMT/FAU-type zeolite nanocrystal aggregates in high yield and crystalline form" C. R. Chimie 19 (2016) 475-465.
4. B. Sowerby, B.D. Crittenden. "An Experimental Comparison of Type A Molecular Sieves for Drying the Ethanol-Water Azeotrope". Gas Separation & Purification 2 (1988) 77-83.
5. E. Gabrus, et al. "Experimental studies on 3A and 4A zeolite molecular sieves regeneration in TSA process: Aliphatic alcohols dewatering–water desorption". Chem. Eng. J. 259 (2015) 232–242.
6. G. Mousa, J.-Ch. Buhl. "Synthesis and characterization of zeolite A by hydrothermal transformation of natural Jordanian kaolin" Journal of the Association of Arab Universities for Basic and Applied Sciences 15 (2014) 35–42.
7. R. Chaiwat, O. Khajornsak "Modification of Synthetic Zeolite Pellets from Lignite Fly Ash A : The Pelletization".World of Coal Ash (WOCA) (2007) 7-10.
8. W. Jens, E. Stefan, G. Bernd, D. Wolf-Dieter "Separation of gaseous water/ethanol mixtures by adsorption on hydrophobic zeolites" ZEOLITES 11 (1991) 314-317.
9. M. Simo, S. Sivashanmugam, C. J. Brown and V. Hlavacek "Adsorption/Desorption of Water and Ethanol on 3A Zeolite in Near-Adiabatic Fixed Bed" Ind. Eng. Chem. Res. 48 (2009) 9247–9260
10. K. E. Strawhecker and E. Manias "Structure and Properties of Poly(vinyl alcohol)/Na+ Montmorillonite Nanocomposites" Chem. Mater. 2000, 12, 2943-2949

11. S. Rimdusit, S. Jingjid, S. Damrongsakkul, S. Tiptipakorn, T. Takeichi "Biodegradability and property characterizations of Methyl Cellulose: Effect of nanocompositing and chemical crosslinking" Carbohydrate Polymers 72 (2008) 444–455
12. S. Authayanun, W. Pothong, D. Saebea, Y. Patcharavorachot, A. Arpornwichanop "Modeling of an industrial fixed bed reactor based on lumped kinetic models for hydrogenation of pyrolysis gasoline" Journal of Industrial and Engineering Chemistry 14 (2008) 771–778
13. T. Aida, D. Na-Ranong, R. Kobayashi, H. Niiyama "Effect of diffusion and adsorption-desorption on periodic operation performance of NO-CO reaction over supported noble metal catalysts" Chemical Engineering Science 54 (1999) 4449-4457
14. G. Rioland, T. J. Daou, D. Faye, J. Patarin "A new generation of MFI-type zeolite pellets with very high mechanical performance for space decontamination" Microporous and Mesoporous Materials 221 (2016) 167-174
15. R. Hernández-Montelongoa, J. P. García-Sandovala, A. González-Álvareza, D. Dochainb, E. Aguilar-Garnicac, "Biodiesel production in a continuous packed bed reactor with recycle: a modeling approach for an esterification system" Renewable Energy 116 (2018) 857-865
16. L. Wang, G. Chen, J. Tang, M. Ming, C. Jia, B. Feng "Continuous biosynthesis of geranyl butyrate in a circulating fluidized bed reactor" Food Bioscience 27 (2019) 60-67
17. J. Mal, Y. V. Nancharaiah, N. Maheshwari, E. D.van, H. Piet, N. L. Lens "Continuous removal and recovery of tellurium in an up flow anaerobic granular sludge bed reactor" Journal of Hazardous Materials 327 (2017) 79-88
18. M.E.E. Abashar, A.A. Al-Rabiah "Investigation of the efficiency of sorption-enhanced methanol synthesis process in circulating fast fluidized bed reactors" Fuel Processing Technology 179 (2018) 387-398
19. D.A. Fedosov, A.V. Smirnov, V.V. Shkirsky, T. Voskoboynikov, I.I. Ivanova "Methanol Dehydration in NaA Zeolite Membrane Reactor" Journal of Membrane Science 486 (2015) 189-194

20. H. Ham, J. Kim, J. H. Lim, W. C. Sung, D. H. Lee, J. W. Bae "Selective ethanol synthesis via multi-step reactions from syngas: Ferrierite-based catalysts and fluidized-bed reactor application" Catalysis Today 303 (2018) 93-99

21. V.J. Inglezakisa, M.M. Fyrillasb, M.A. Stylianouc "Two-phase homogeneous diffusion model for the fixed bed sorption of heavy metals on natural zeolites" Microporous and Mesoporous Materials 266 (2018) 164-176

22. S. Yaghoobi-Khankhajeh, R. Alizadeh, R. Zarghami "Adsorption modeling of CO_2 in fluidized bed reactor" Chemical Engineering Research and Design 129 (2018) 111-121

23. M. Wenzel, L. Rihko-Struckmann, K. Sundmacher "Continuous production of CO from CO_2 by RWGS chemical looping in fixed and fluidized bed reactors" Chemical Engineering Journal 336 (2018) 278-296

24. G. Xu, X. Zhang, Z. Sun, J. Ruan, B. He "Flow patterns and transition criteria in boiling water-cooled packed bed reactors" Progress in Nuclear Energy 108 (2018) 214-221

25. N. de Nooijer, F. Gallucci, E. Pellizzari, J. Melendez, D. Alfredo, P. Tanaka, G. Manzolini, M. van, S. Annaland "On concentration polarisation in a fluidized bed membrane reactor for biogas steam reforming: Modelling and experimental validation" Chemical Engineering Journal 348 (2018) 232-243

26. C.D. Lane, C.A. McKnight, J. Wiens, K. Reid, A.A. Donaldson "Parametric analysis of internal gas separation within an ebullated bed reactor" Chemical Engineering Research and Design 105 (2016) 44–54

27. J. Freiding, F.C. Patcas, B. Kraushaar-Czarnetzki "Extrusion of zeolites: Properties of catalysts with a novel aluminium phosphate sintermatrix" Applied Catalysis A: General 328 (2007) 210–218

28. D.P. Serrano, R. Sanz, P. Pizarro, I. Moreno, P. de Frutos, S. Bla´zquez "Preparation of extruded catalysts based on TS-1 zeolite for their application in propylene epoxidation" Catalysis Today 143 (2009) 151-157

29. I. Bezverkhyy, K. Bouguessa, C. Geantet, M. Vrinat "Adsorption of tetrahydrothiophene on faujasite type zeolites : Breakthrough curves and FTIR spectroscopy study" Applied Catalysis B : Environmental 62 (2006) 299–305

30. D. Ferreira, R. Magalhaes, P. Taveira, A. Mendes "Effective Adsorption Equilibrium Isotherms and Breakthroughs of Water Vapor and Carbon Dioxide on Different Absorbents" Ind. Eng. Chem. Res. 50 (2011) 10201–10210

31. S. Karimi, B. Ghobadian, M.R. Omidkhah, J. Towfighi, M. T. Yaraki "Experimental investigation of bioethanol liquid phase dehydration using natural clinoptilolite" Journal of Advanced Research 7 (2016) 435–444

32. J. Weitkamp, S. Ernst, B. Giinzel, W.D. Deckwer "Separation of gaseous water/ethanol mixtures by adsorption on hydrophobic zeolites" ZEOLITES 11 (1991) 314-317

APPENDICES

Appendix A: GPC Results

Figure A.1-A.6 using Gel Permeation Chromatography (GPC)

Table A.1-A.6 using Gel Permeation Chromatography (GPC)

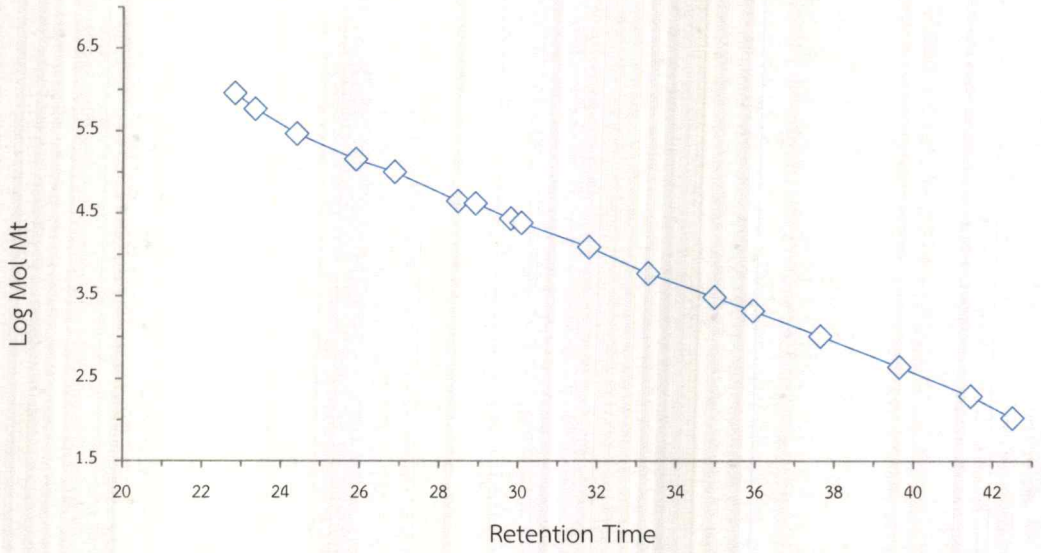

Figure A.1 Calibration for GPC result of PVA JP-27, PVA GL-05 and PVA NL-05

Table A.1 Calibration for GPC result of PVA JP-27, PVA GL-05 and PVA NL-05

	1	2	3	4	5	6	7	8
Retention Time	22.833	23.339	24.391	25.888	26.868	28.471	28.919	29.806
Elution Volume	22.833	23.339	24.391	25.888	26.868	28.471	28.919	29.806
Mol Wt	903000	580000	290000	143000	101000	44200	41300	27000
Log Mol Wt	5.956	5.763	5.462	5.155	5.004	4.645	4.616	4.431
Calculated Weight	793785.805	594447.129	333970.757	155050.453	96600.518	46401.272	38118.024	26011.735
% Residual	13.758	-2.430	-13.166	-7.772	4.554	-4.744	8.348	3.799
Result Id	1500	1503	1504	1500	1503	1500	1505	1503
Channel Id	1103	1106	1111	1103	1106	1103	1097	1106

	9	10	11	12	13	14	15	16	17
Retention Time	30.071	31.791	33.289	34.971	35.943	37.65	39.643	41.443	42.501
Elution Volume	30.071	31.791	33.289	34.971	35.943	37.65	39.643	41.443	42.501
Mol Wt	24100	12200	5890	3060	2090	1020	434	194	106
Log Mol Wt	4.382	4.086	3.770	3.486	3.320	3.009	2.637	2.288	2.025
Calculated Weight	23248 .589	11402 .372	6220 .006	3158 .908	2125 .890	1043 .031	433 .988	184 .956	108 .278
% Residual	3.662	6.995	-5.305	-3.131	-1.689	-2.208	0.003	4.888	-2.104
Result Id	1507	1505	1507	1505	1507	1505	1507	1505	1507
Channel Id	1100	1097	1100	1097	1100	1097	1100	1097	1100

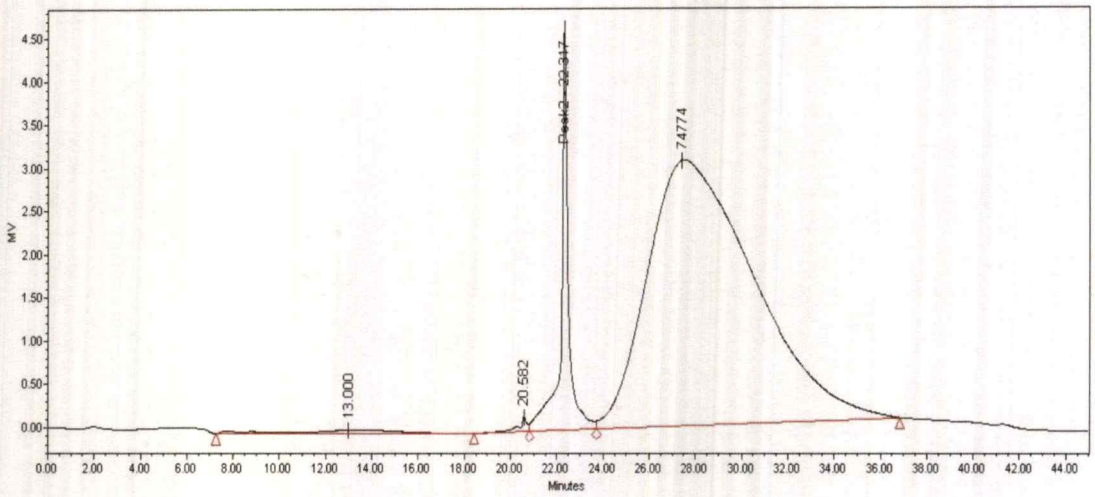

Figure A.2 GPC result of PVA JP-27

Table A.2 GPC result of PVA JP-27

Name			Peak 2		Broad
Retention time	13	20.582	22.317	27.417	32.668
Peak Codes	I08 G11	G11	G11	I08	
Mn (Daltons)			907310		
Mw (Daltons)			935456		
MP (Daltons)				74774	
Mv (Daltons)					
Mz (Daltons)			956663		
Mz+1 (Daltons)			972518		
Polydisperity			1.031022		
Mz/Mw			1.022670		
Mz+1/Mw			1.039618		
Id	0	0	0	0	0
Area	14759	4831	103467	988926	
% Area	1.33	0.43	9.3	88.93	
Height	44	168	4634	3080	
Int Type	BB	BV	VV	VB	Miss

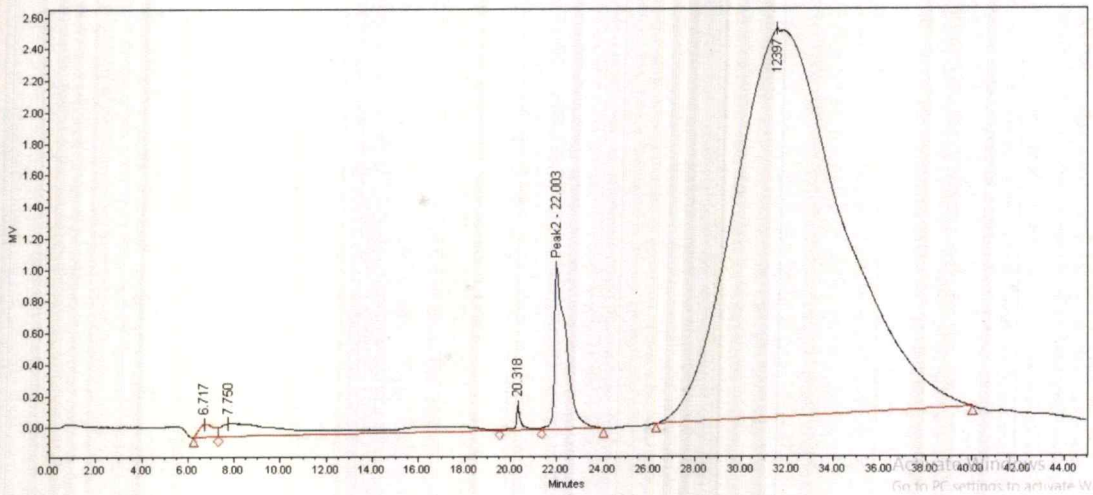

Figure A.3 GPC result of PVA GL-05

Table A.3 GPC result of PVA GL-05

Name				Peak 2	Broad
Retention time	6.717	7.75	20.318	22.003	31.587
Peak Codes	I08 G11	I08 G11	G11	G11	
Mn (Daltons)				894456	5746
Mw (Daltons)				917819	13475
MP (Daltons)					12397
Mv (Daltons)					
Mz (Daltons)				936314	24803
Mz+1 (Daltons)				951023	38572
Polydisperity				1.026120	2.345291
Mz/Mw				1.020151	1.840622
Mz+1/Mw				1.036176	2.862466
Id	0	0	0	1520	1521
Area	3817	26414	2557	36592	792281
% Area	0.44	3.07	0.3	4.25	91.95
Height	83	85	152	1026	2457
Int Type	BV	VV	VV	VB	BB

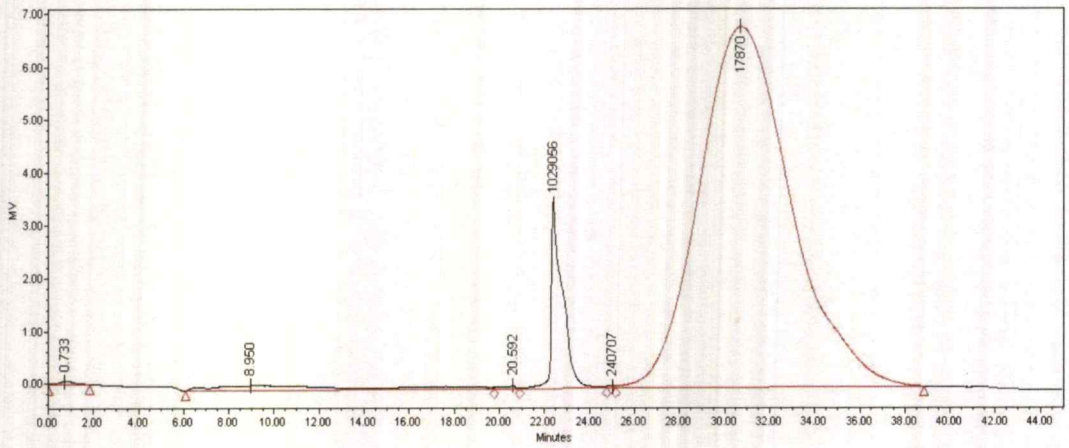

Figure A.4 GPC result of PVA NL-05

Table A.4 GPC result of PVA NL-05

Name				Peak 2		Broad
Retention time	0.733	8.95	20.592	22.391	25.017	30.7
Peak Codes	I08 G11	I08 G11	G11		I08	I08
Mn (Daltons)				825873		10766
Mw (Daltons)				860307		21024
MP (Daltons)				1029056	240407	17870
Mv (Daltons)						
Mz (Daltons)				886178		36971
Mz+1 (Daltons)				906701		61397
Polydisperity				1.041694		1.952757
Mz/Mw				1.030072		1.758527
Mz+1/Mw				1.053927		2.920309
Id	0	0	0	1515	0	1516
Area	3623	39923	1917	122984	820	1918378
% Area	0.17	1.91	0.09	5.89	0.04	91.89
Height	67	88	65	3536	37	6822
Int Type	BB	BV	VV	VV	VV	VB

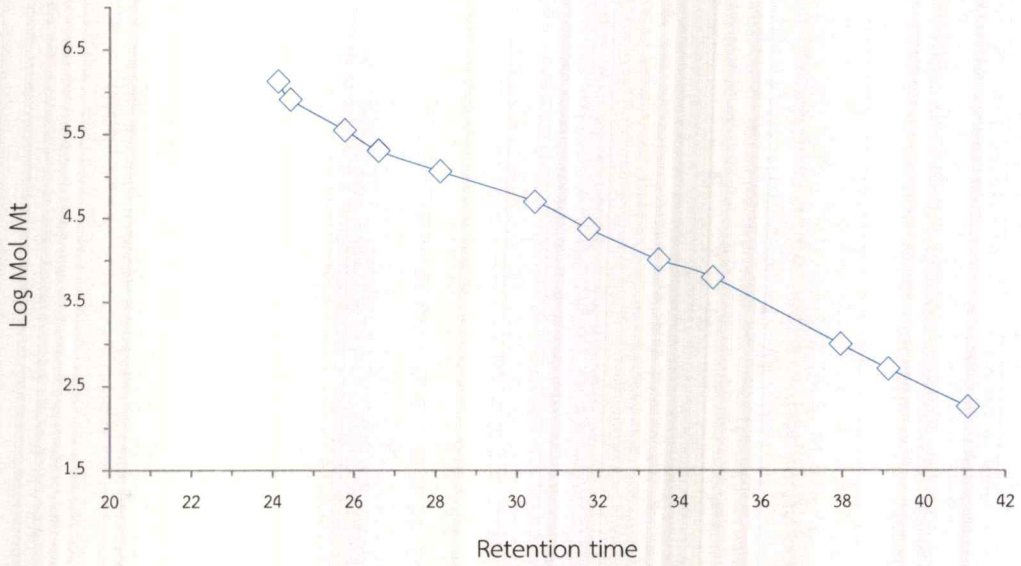

Figure A.5 Calibration for GPC result of Methylcellulose

Table A.5 Calibration for GPC result of Methylcellulose

	1	2	3	4	5	6
Retention Time	24.133	24.433	25.767	26.592	28.113	30.436
Elution Volume	24.133	24.433	25.767	26.592	28.113	30.436
Mw	1330000	805000	348000	200000	113000	48800
Log Mw	6.1238	5.9057	5.5415	5.3010	5.0530	4.6884
Calculated Weight	1042320	863111	392641	250143	115695	39477
% Residual	27.600	-6.733	-11.370	-20.046	-2.330	23.616
Result Id	3845	3846	3842	3845	3846	3842
Channel Id	3711	3717	3769	3711	3717	3769

	7	8	9	10	11	12
Retention Time	31.765	33.486	34.814	37.957	39.131	41.079
Elution Volume	31.765	33.486	34.814	37.957	39.131	41.079
Mol Wt	23000	10000	6200	991	504	180
Log Mol Wt	4.3617	4.000	3.7923	2.9960	2.7024	2.2552
Calculated Weight	21965	10276	5610	1138	573	158
% Residual	4.713	-2.681	10.525	-12.904	-12.035	13.814
Result Id	3845	3846	3842	3845	3846	3842
Channel Id	3711	3717	3769	3711	3717	3769

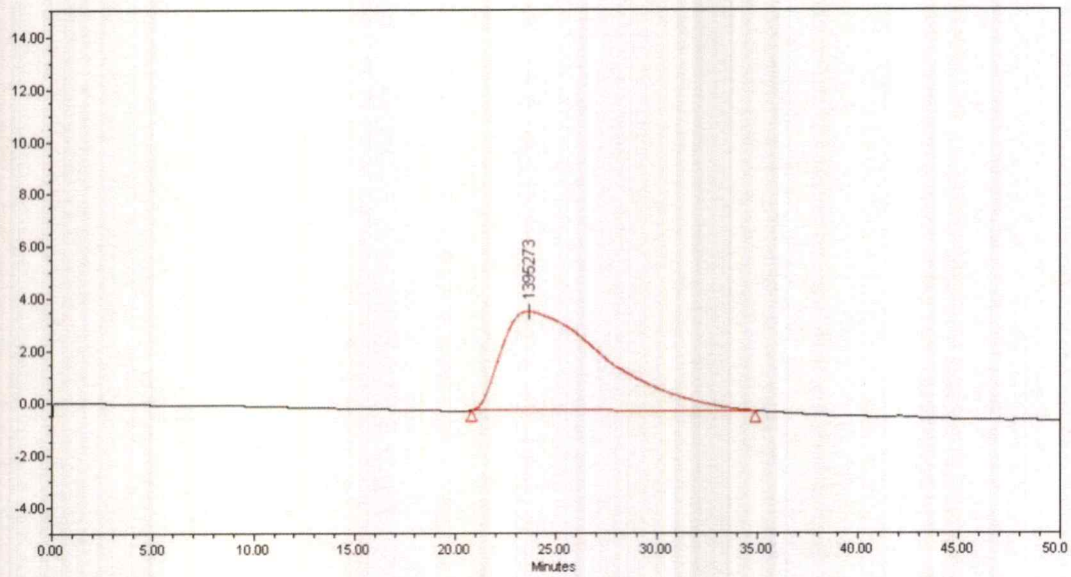

Figure A.6 GPC result of Methylcellulose

Table A.6 GPC result of Methylcellulose

Name	Peak 2
Retention time	23.683
Peak Codes	I08 G39
Mn (Daltons)	163026
Mw (Daltons)	1067012
MP (Daltons)	1395273
Mv (Daltons)	
Mz (Daltons)	2688304
Mz+1 (Daltons)	410388
Polydisperity	6.545027
Mz/Mw	2.519468
Mz+1/Mw	3.842868
Id	0
Area	1365390
% Area	100
Height	3810
Int Type	BB

Appendix B: TGA Results

Figure B.1-B.8 using Thermal gravimetric analysis (TGA)

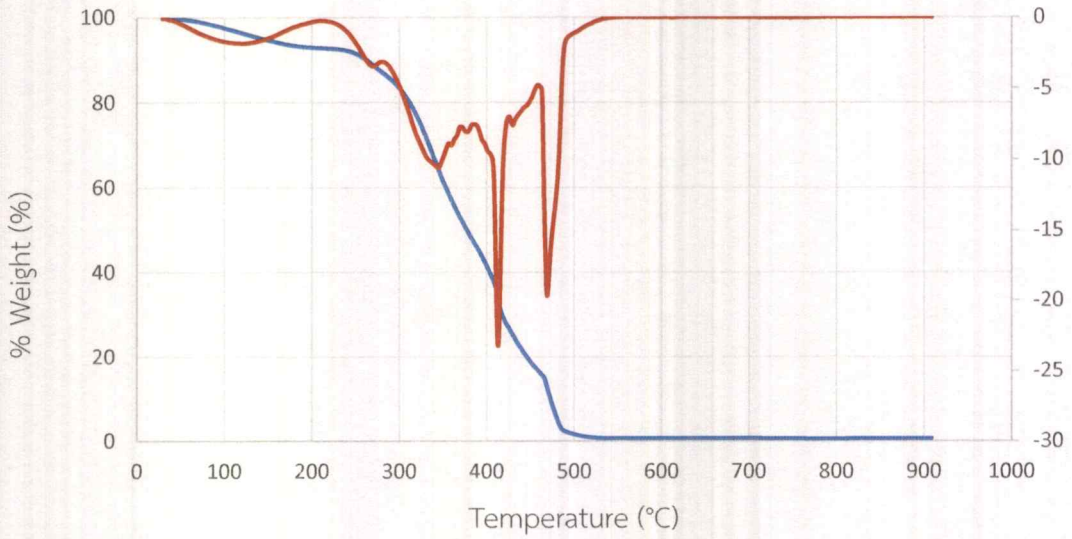

Figure B.1 TGA profiles for PVA JP-27

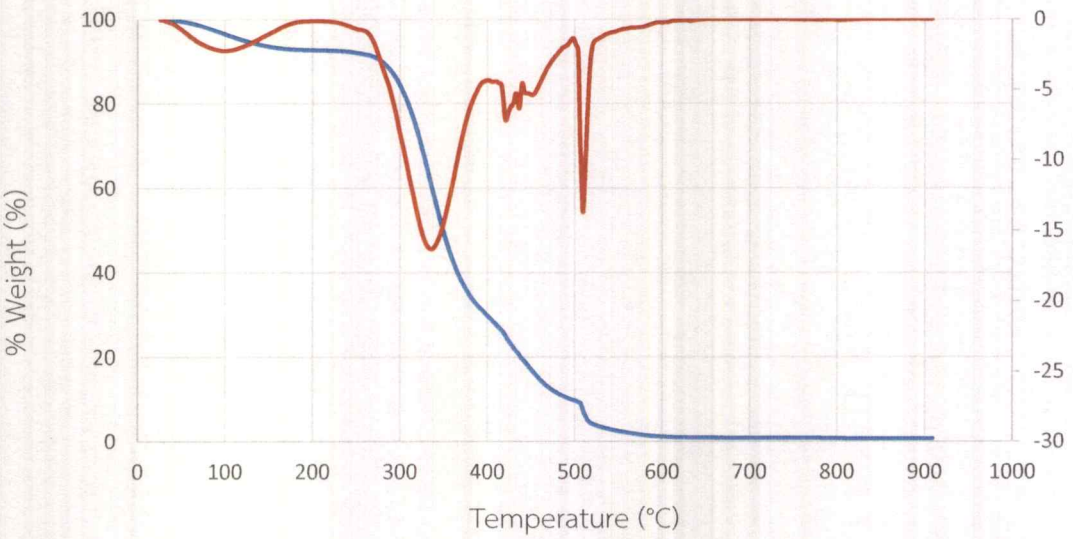

Figure B.2 TGA profiles for PVA GL-05

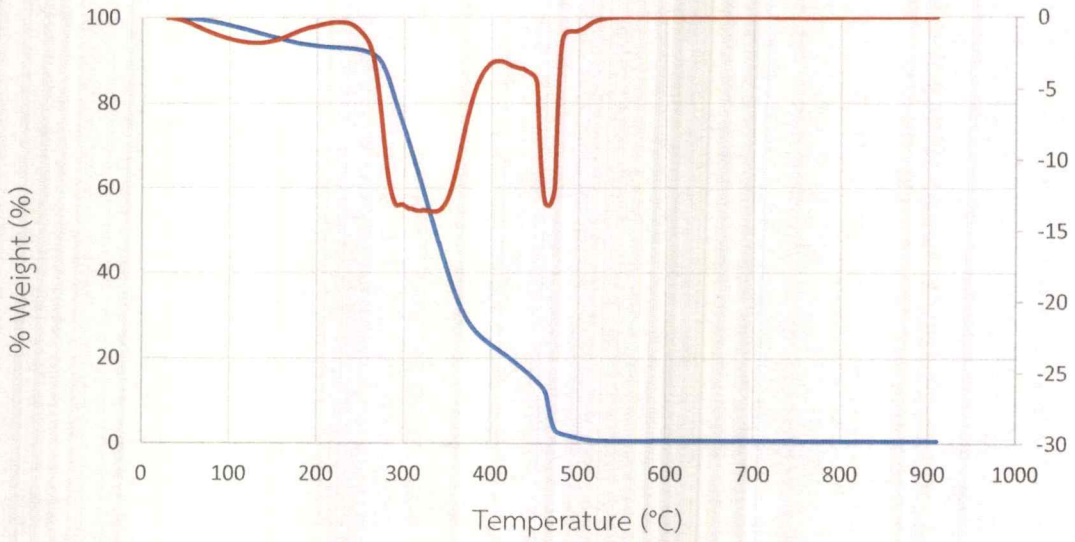

Figure B.3 TGA profiles for PVA NL-05

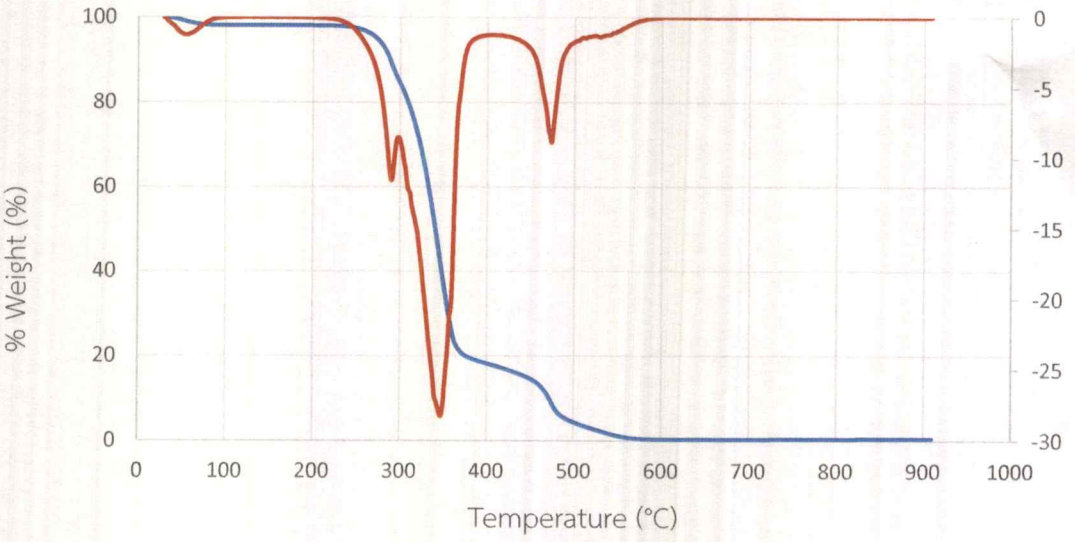

Figure B.4 TGA profiles for MC

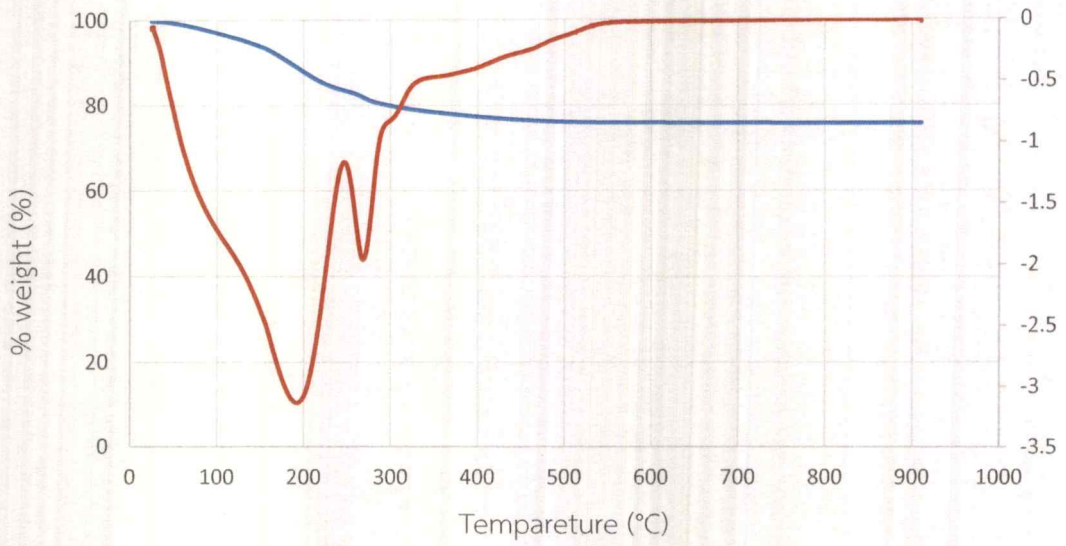

Figure B.5 TGA profiles for Z-PVA JP-27

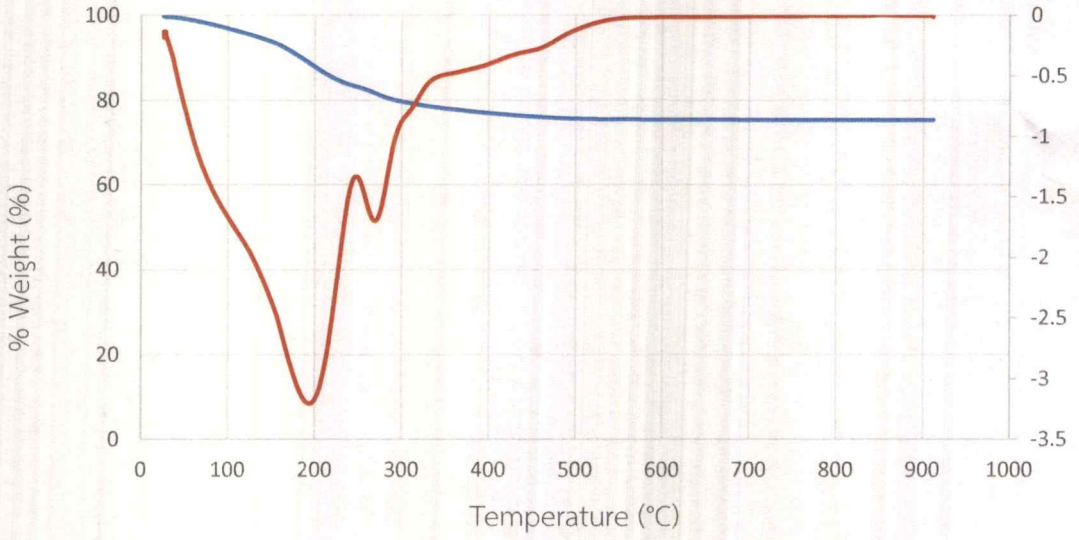

Figure B.6 TGA profiles for Z-PVA GL-05

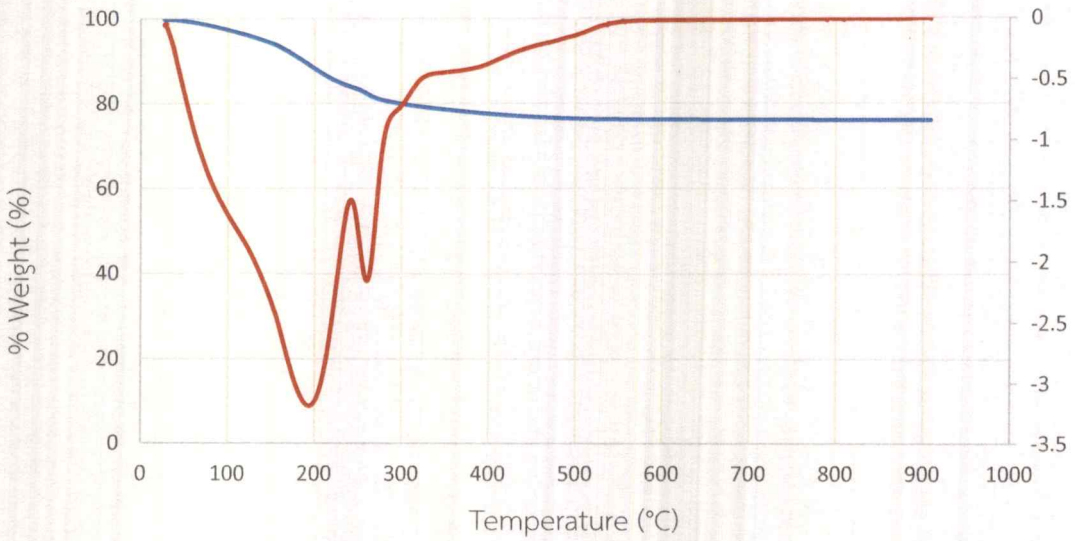

Figure B.7 TGA profiles for Z-PVA NL-05

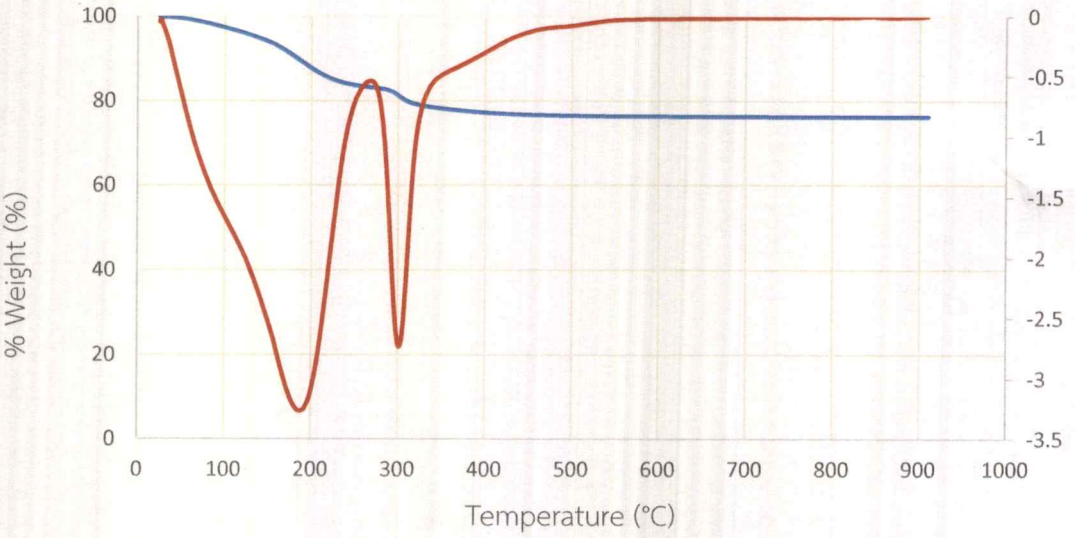

Figure B.8 TGA profiles for Z-MC

Appendix C: GC-TCD Results

Figure C.1-C.18 using Gas Chromatography –Thermal Conductivity Detector (GC-TCD)

Table C.1-C.18 using Gas Chromatography –Thermal Conductivity Detector (GC-TCD)

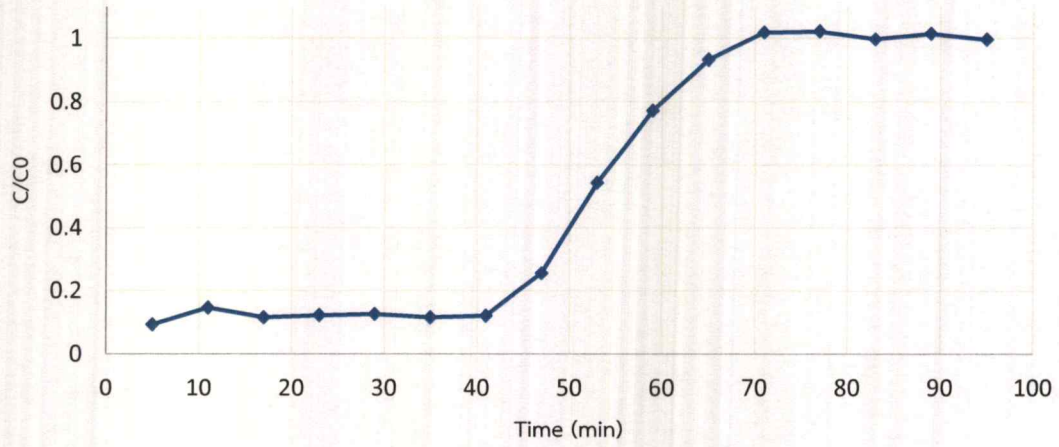

Figure C.1 Breakthrough curve of Zeolite-PVA JP-27 95% EtOH, pack 5 cm, feed 2 ml/h, N_2 flow 20 ml/min (30 min activation)

Table C.1 Breakthrough curve of Zeolite-PVA JP-27 95% EtOH, pack 5 cm, feed 2 ml/h, N_2 flow 20 ml/min (30 min activation)

	% Area water	Time	% Water	C/C0
Initial	13.352	-	4.825828	0.999999
1	1.245	5	0.449978	0.093244
2	1.952	11	0.705508	0.146194
3	1.547	17	0.559130	0.115862
4	1.635	23	0.590935	0.122453
5	1.684	29	0.608645	0.126122
6	1.544	35	0.558045	0.115637
7	1.613	41	0.582984	0.120805
8	3.421	47	1.236446	0.256214
9	7.248	53	2.619633	0.542836
10	10.298	59	3.721989	0.771264
11	12.448	65	4.499060	0.932288
12	13.594	71	4.913257	1.018117

Table C.1 Continue

13	13.642	77	4.930606	1.021712
14	13.315	83	4.812419	0.997221
15	13.541	89	4.894101	1.014148
16	13.298	95	4.806274	0.995948

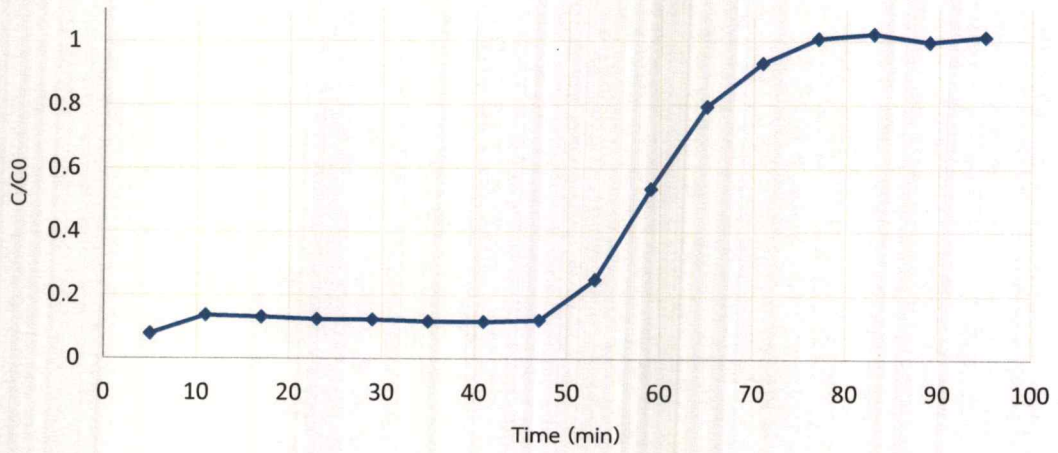

Figure C.2 Breakthrough curve of Zeolite-PVA JP-27 95% EtOH, pack 8 cm, feed 2 ml/h, N_2 flow 20 ml/min (30 min activation)

Table C.2 Breakthrough curve of Zeolite-PVA JP-27 95% EtOH, pack 8 cm, feed 2 ml/h, N_2 flow 20 ml/min (30 min activation)

	% Area water	Time	% Water	C/C0
Initial	13.352	-	4.825828	0.999999
1	1.032	5	0.372994	0.077291
2	1.821	11	0.658161	0.136383
3	1.746	17	0.631054	0.130766
4	1.656	23	0.598525	0.124025
5	1.643	29	0.593827	0.123052
6	1.568	35	0.56672	0.117435
7	1.556	41	0.562383	0.116536
8	1.629	47	0.588767	0.122003
9	3.341	53	1.207532	0.250223
10	7.158	59	2.587104	0.536095
11	10.605	65	3.832948	0.794257
12	12.423	71	4.490025	0.930415
13	13.450	77	4.861212	1.007332
14	13.640	83	4.929883	1.021562
15	13.299	89	4.806636	0.996023
16	13.513	95	4.883981	1.012050

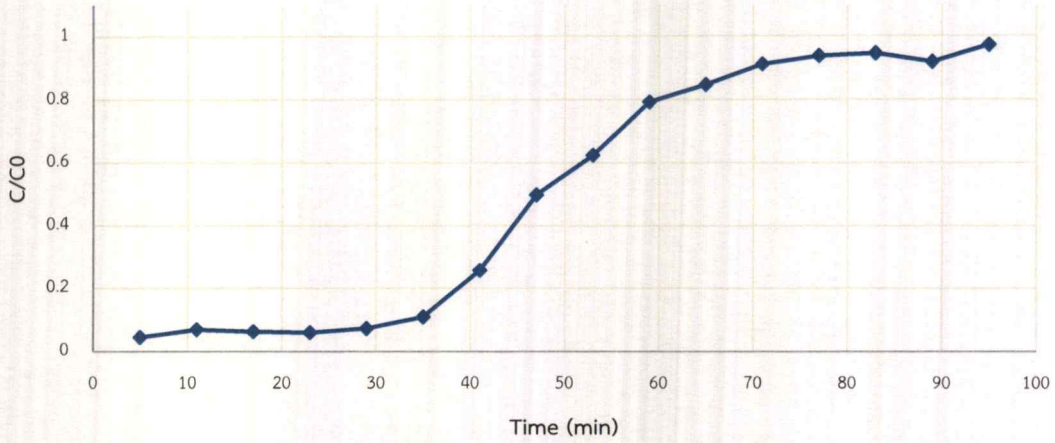

Figure C.3 Breakthrough curve of Zeolite-PVA JP-27 95% EtOH, pack 8 cm, feed 2 ml/h, N_2 flow 20 ml/min (30 min activation)

Table C.3 Breakthrough curve of Zeolite-PVA JP-27 95% EtOH, pack 8 cm, feed 2 ml/h, N_2 flow 20 ml/min (30 min activation)

	% Area water	Time	% Water	C/C0
Initial	13.352	-	4.825828	0.999999
1	0.606	5	0.219026	0.045386
2	0.928	11	0.335406	0.069502
3	0.846	17	0.305768	0.063361
4	0.802	23	0.289866	0.060065
5	0.974	29	0.352031	0.072947
6	1.464	35	0.529131	0.109646
7	3.441	41	1.243675	0.257712
8	6.652	47	2.404221	0.498199
9	8.327	53	3.009614	0.623647
10	10.579	59	3.823551	0.792310
11	11.308	65	4.087032	0.846908
12	12.169	71	4.398222	0.911392
13	12.510	77	4.521469	0.936931
14	12.616	83	4.559780	0.944870
15	12.260	89	4.431112	0.918208
16	12.963	95	4.685196	0.970858

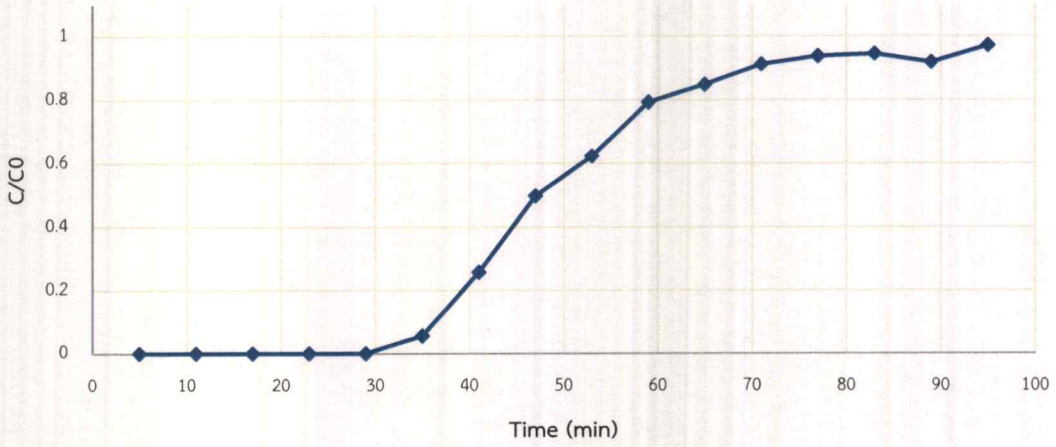

Figure C.4 Breakthrough curve of Zeolite-PVA JP-27 95% EtOH, pack 8 cm, feed 2 ml/h, N_2 flow 10 ml/min (30 min activation)

Table C.4 Breakthrough curve of Zeolite-PVA JP-27 95% EtOH, pack 8 cm, feed 2 ml/h, N_2 flow 10 ml/min (30 min activation)

	% Area water	Time	% Water	C/C0
Initial	12.572	-	4.543841	0.999999
1	0	5	0	0
2	0	11	0	0
3	0	17	0	0
4	0	23	0	0
5	0	29	0	0
6	0.735	35	0.26565	0.055048
7	3.441	41	1.243675	0.257712
8	6.652	47	2.404221	0.498199
9	8.327	53	3.009614	0.623647
10	10.579	59	3.823551	0.792310
11	11.308	65	4.087032	0.846908
12	12.169	71	4.398222	0.911392
13	12.510	77	4.521469	0.936931
14	12.616	83	4.55978	0.944870
15	12.260	89	4.431112	0.918208
16	12.963	95	4.685196	0.970858

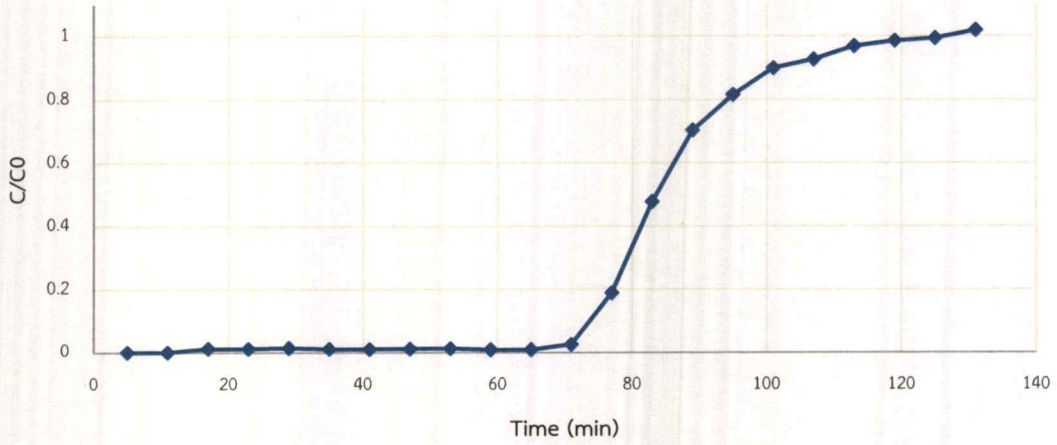

Figure C.5 Breakthrough curve of Zeolite-PVA JP-27 95% EtOH, pack 8 cm, feed 2 ml/h, N_2 flow 10 ml/min (60 min desorption)

Table C.5 Breakthrough curve of Zeolite-PVA JP-27 95% EtOH, pack 8 cm, feed 2 ml/h, N_2 flow 10 ml/min (60 min desorption)

	% Area water	Time	% Water	C/C0
Initial	13.352	-	4.825828	0.999999
1	0	5	0	0
2	0	11	0	0
3	0.158	17	0.057106	0.011833
4	0.154	23	0.05566	0.011534
5	0.188	29	0.067949	0.014080
6	0.145	35	0.052407	0.010860
7	0.143	41	0.051684	0.010710
8	0.150	47	0.054214	0.011234
9	0.163	53	0.058913	0.012208
10	0.114	59	0.041203	0.008538
11	0.113	65	0.040841	0.008463
12	0.331	71	0.119633	0.024790
13	2.513	77	0.908269	0.188210
14	6.380	83	2.305913	0.477827
15	9.395	89	3.395619	0.703635
16	10.892	95	3.936678	0.815752

Table C.5 Continue

17	12.01	101	4.340755	0.899484
18	12.369	107	4.470507	0.926371
19	12.925	113	4.671462	0.968012
20	13.154	119	4.754229	0.985163
21	13.258	125	4.791817	0.992952
22	13.603	131	4.91651	1.018791
23	13.499	137	4.878921	1.011002

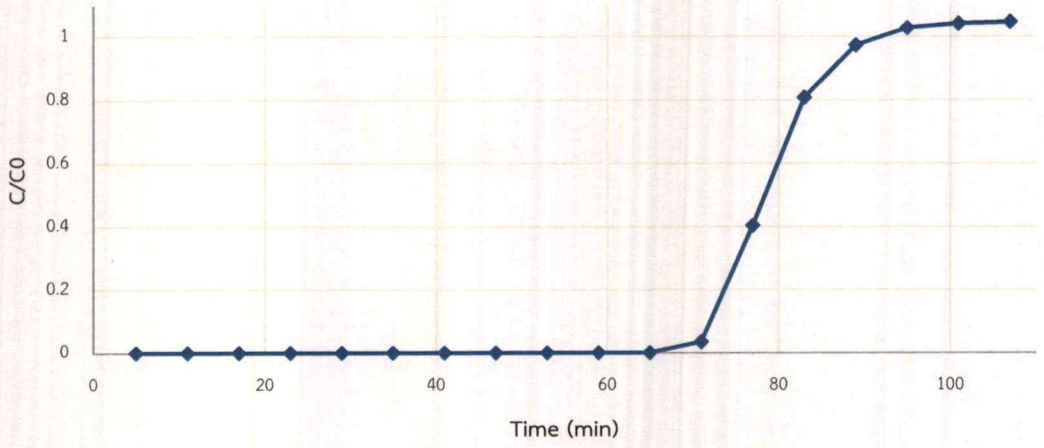

Figure C.6 Breakthrough curve of Zeolite-PVA JP-27 95% EtOH, pack 8 cm, feed 2 ml/h, N_2 flow 10 ml/min (90 min desorption)

Table C.6 Breakthrough curve of Zeolite-PVA JP-27 95% EtOH, pack 8 cm, feed 2 ml/h, N_2 flow 10 ml/min (90 min desorption)

	% Area water	Time	% Water	C/C0
Initial	14.233	-	5.14421	1
1	0	5	0	0
2	0	11	0	0
3	0	17	0	0
4	0	23	0	0
5	0	29	0	0
6	0	35	0	0
7	0	41	0	0
8	0	47	0	0
9	0	53	0	0
10	0	59	0	0
11	0	65	0	0
12	0.487	71	0.176016	0.034216
13	5.754	77	2.079659	0.404272
14	11.499	83	4.156065	0.807911
15	13.840	89	5.002169	0.972388
16	14.627	95	5.286613	1.027682

Table C.6 Continue

17	14.820	101	5.356368	1.041242
18	14.887	107	5.380584	1.04595

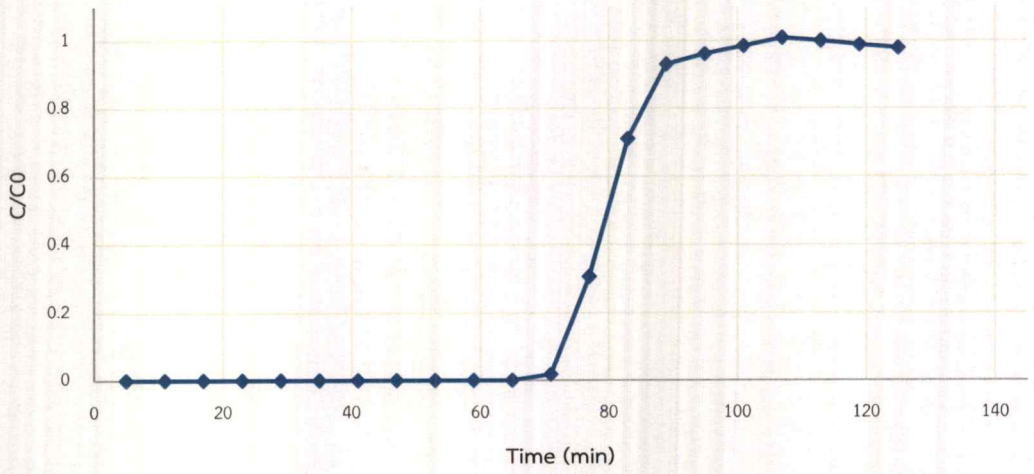

Figure C.7 Breakthrough curve of Zeolite-PVA JP-27 95% EtOH, pack 8 cm, feed 2 ml/h, N_2 flow 10 ml/min (60 min activation)

Table C.7 Breakthrough curve of Zeolite-PVA JP-27 95% EtOH, pack 8 cm, feed 2 ml/h, N_2 flow 10 ml/min (60 min activation)

	% Area water	Time	% Water	C/C0
Initial	14.12	-	5.103548	1
1	0	5	0	0
2	0	11	0	0
3	0	17	0	0
4	0	23	0	0
5	0	29	0	0
6	0	35	0	0
7	0	41	0	0
8	0	47	0	0
9	0	53	0	0
10	0	59	0	0
11	0	65	0	0
12	0.249	71	0.089996	0.017634
13	4.323	77	1.562455	0.306151
14	10.028	83	3.624404	0.710173
15	13.146	89	4.751337	0.930987
16	13.572	95	4.905306	0.961156

Table C.7 Continue

17	13.900	101	5.023854	0.984385
18	14.243	107	5.147824	1.008676
19	14.121	113	5.10373	1.000036
20	13.955	119	5.043733	0.988280
21	13.822	125	4.995663	0.978861

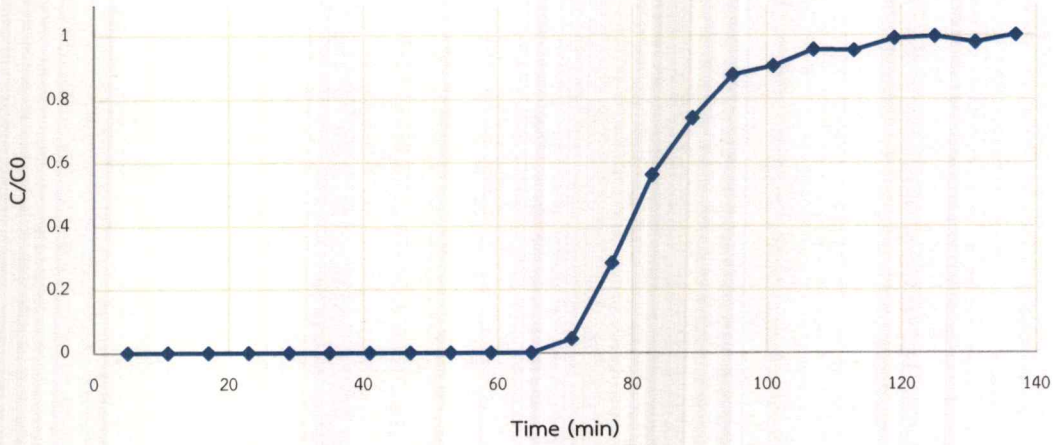

Figure C.8 Breakthrough curve of Zeolite-PVA GL-05 95% EtOH, pack 8 cm, feed 2 ml/h, N_2 flow 10 ml/min (60 min activation)

Table C.8 Breakthrough curve of Zeolite-PVA GL-05 95% EtOH, pack 8 cm, feed 2 ml/h, N_2 flow 10 ml/min (60 min activation)

	% Area water	Time	% Water	C/C0
Initial	14.233	-	5.14421	1
1	0	5	0	0
2	0	11	0	0
3	0	17	0	0
4	0	23	0	0
5	0	29	0	0
6	0	35	0	0
7	0	41	0	0
8	0	47	0	0
9	0	53	0	0
10	0	59	0	0
11	0	65	0	0
12	0.627	71	0.226616	0.044053
13	4.042	77	1.460893	0.283988
14	8.000	83	2.891427	0.562074
15	10.553	89	3.814154	0.741446
16	12.470	95	4.507012	0.876133

Table C.8 Continue

17	12.872	101	4.652306	0.904377
18	13.604	107	4.916871	0.955807
19	13.569	113	4.904221	0.953348
20	14.110	119	5.099754	0.991358
21	14.195	125	5.130476	0.997330
22	13.931	131	5.035059	0.978782
23	14.262	137	5.154691	1.002038

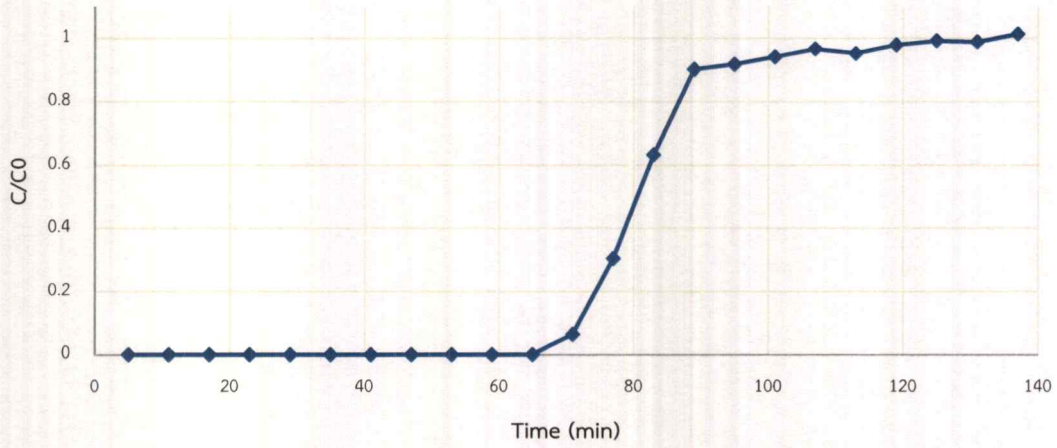

Figure C.9 Breakthrough curve of Zeolite-PVA NL-05 95% EtOH, pack 8 cm, feed 2 ml/h, N_2 flow 10 ml/min (60 min activation)

Table C.9 Breakthrough curve of Zeolite-PVA NL-05 95% EtOH, pack 8 cm, feed 2 ml/h, N_2 flow 10 ml/min (60 min activation)

	% Area water	Time	% Water	C/C0
Initial	12.7	-	4.589741	1
1	0	5	0	0
2	0	11	0	0
3	0	17	0	0
4	0	23	0	0
5	0	29	0	0
6	0	35	0	0
7	0	41	0	0
8	0	47	0	0
9	0	53	0	0
10	0	59	0	0
11	0	65	0	0
12	0.807	71	0.291673	0.063549
13	3.880	77	1.402342	0.305538
14	8.043	83	2.906968	0.633362
15	11.455	89	4.140162	0.902047
16	11.652	95	4.211363	0.917560

Table C.9 Continue

17	11.957	101	4.321599	0.941578
18	12.276	107	4.436895	0.966698
19	12.093	113	4.370753	0.952288
20	12.441	119	4.496530	0.979692
21	12.603	125	4.555082	0.992449
22	12.559	131	4.539179	0.988984
23	12.875	137	4.653390	1.013868

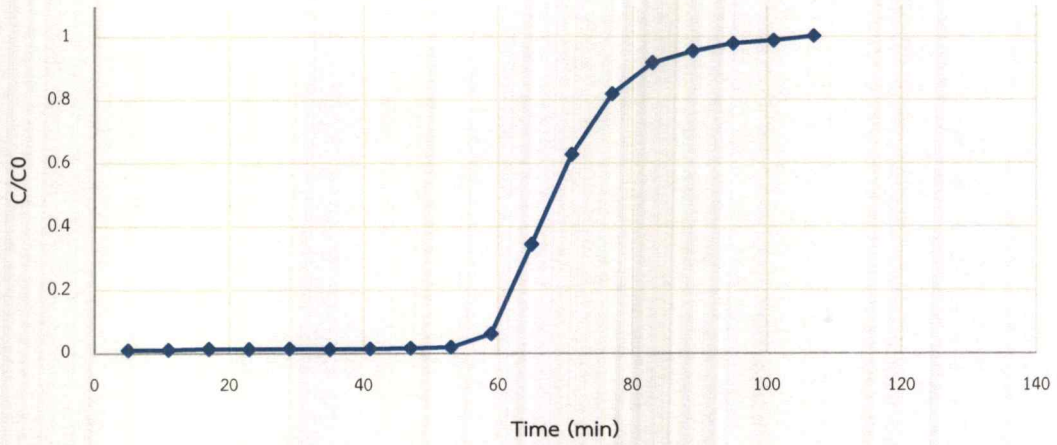

Figure C.10 Breakthrough curve of Zeolite-MC 95% EtOH, pack 8 cm, feed 2 ml/h, N_2 flow 10 ml/min (60 min activation)

Table C.10 Breakthrough curve of Zeolite-MC 95% EtOH, pack 8 cm, feed 2 ml/h, N_2 flow 10 ml/min (60 min activation)

	% Area water	Time	% Water	C/C0
Initial	13.847	-	5.004875	1
1	0.136	5	0.049154	0.009821
2	0.149	11	0.053853	0.01076
3	0.190	17	0.068671	0.013721
4	0.177	23	0.063973	0.012782
5	0.199	29	0.071924	0.014371
6	0.181	35	0.065419	0.013071
7	0.200	41	0.072286	0.014443
8	0.226	47	0.081683	0.016321
9	0.270	53	0.097586	0.019498
10	0.851	59	0.307576	0.061455
11	4.789	65	1.730880	0.345839
12	8.696	71	3.142981	0.627984
13	11.335	77	4.096791	0.818560
14	12.703	83	4.591225	0.917350
15	13.215	89	4.776276	0.954325
16	13.545	95	4.895547	0.978156

Table C.10 Continue

17	13.674	101	4.942171	0.987472
18	13.882	107	5.017349	1.002492

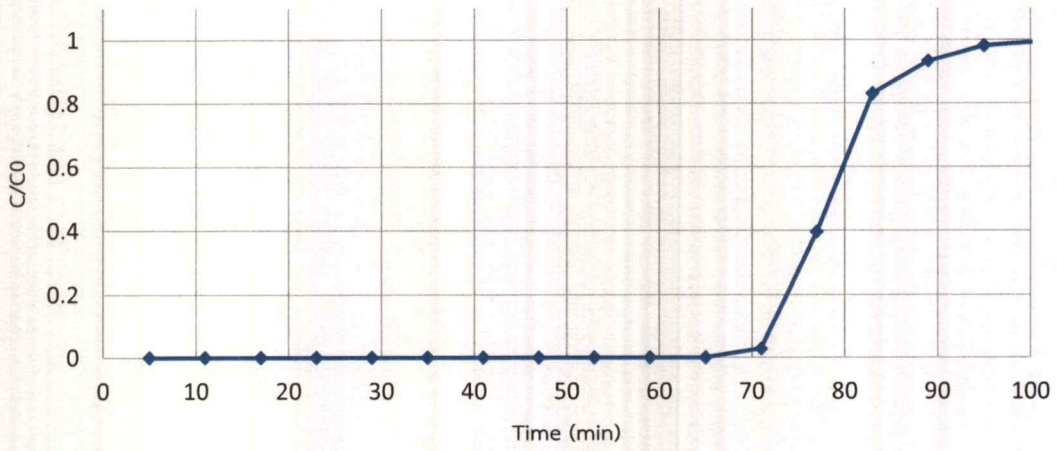

Figure C.11 Breakthrough curve of Zeolite-PVA JP-27 95% EtOH, pack 8 cm, feed 2 ml/h, N_2 flow 10 ml/min (60 min activation)

Table C.11 Breakthrough curve of Zeolite-PVA JP-27 95% EtOH, pack 8 cm, feed 2 ml/h, N_2 flow 10 ml/min (60 min activation)

	% Area water	Time	% Water	C/C0
Initial	11.617	-	4.198745	1
1	0	5	0	0
2	0	11	0	0
3	0	17	0	0
4	0	23	0	0
5	0	29	0	0
6	0	35	0	0
7	0	41	0	0
8	0	47	0	0
9	0	53	0	0
10	0	59	0	0
11	0	65	0	0
12	0.318	71	0.114934	0.027373
13	4.596	77	1.661125	0.395624
14	9.639	83	3.483808	0.829726
15	10.836	89	3.916438	0.932764
16	11.407	95	4.122813	0.981916

Table C.11 Continue

17	11.551	101	4.174859	0.994311
18	11.531	107	4.167630	0.992590
19	11.628	113	4.202689	1.000939
20	11.798	119	4.264132	1.015573
21	11.648	125	4.209918	1.002661

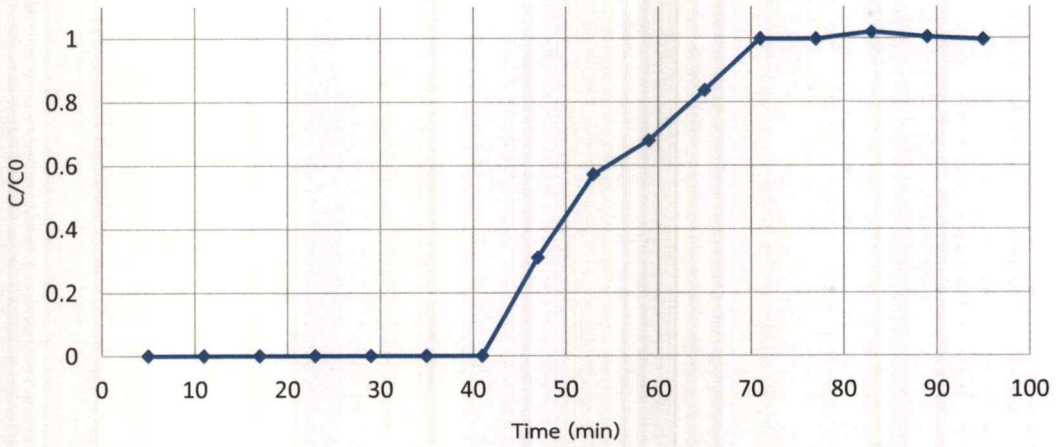

Figure C.12 Breakthrough curve of Zeolite-PVA JP-27 90% EtOH, pack 8 cm, feed 2 ml/h, N_2 flow 10 ml/min (60 min activation)

Table C.12 Breakthrough curve of Zeolite-PVA JP-27 90% EtOH, pack 8 cm, feed 2 ml/h, N_2 flow 10 ml/min (60 min activation)

	% Area water	Time	% Water	C/C0
Initial	28.872	-	10.43516	1
1	0	5	0	0
2	0	11	0	0
3	0	17	0	0
4	0	23	0	0
5	0	29	0	0
6	0	35	0	0
7	0	41	0	0
8	8.942	47	3.231892	0.309712
9	16.502	53	5.964291	0.571557
10	19.573	59	7.074237	0.677923
11	24.162	65	8.732832	0.836866
12	28.811	71	10.41311	0.997887
13	28.789	77	10.40516	0.997125
14	29.436	83	10.63901	1.019534
15	28.972	89	10.4713	1.003464
16	28.754	95	10.39251	0.995913

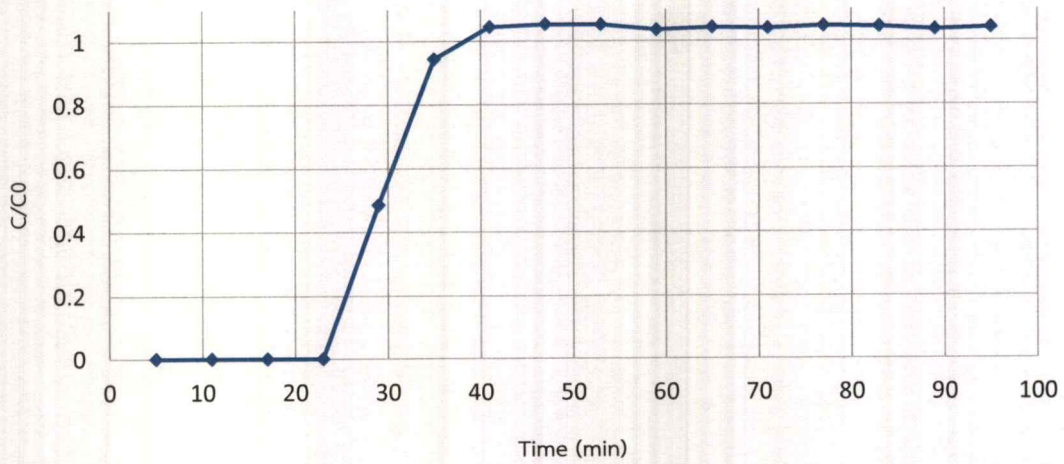

Figure C.13 Breakthrough curve of Zeolite-PVA JP-27 85% EtOH, pack 8 cm, feed 2 ml/h, N_2 flow 10 ml/min (60 min activation)

Table C.13 Breakthrough curve of Zeolite-PVA JP-27 85% EtOH, pack 8 cm, feed 2 ml/h, N_2 flow 10 ml/min (60 min activation)

	% Area water	Time	% Water	C/C0
Initial	45.257	-	16.3571	1
1	0	5	0	0
2	0	11	0	0
3	0	17	0	0
4	0	23	0	0
5	21.099	29	7.625777	0.485648
6	41.019	35	14.82543	0.944159
7	45.442	41	16.42403	1.045966
8	45.802	47	16.55414	1.054252
9	45.734	53	16.52956	1.052687
10	45.015	59	16.26970	1.036137
11	45.339	65	16.38680	1.043595
12	45.216	71	16.34234	1.040764
13	45.531	77	16.45619	1.048014
14	45.442	83	16.42403	1.045966
15	45.034	89	16.27656	1.036575
16	45.294	95	16.37054	1.042559

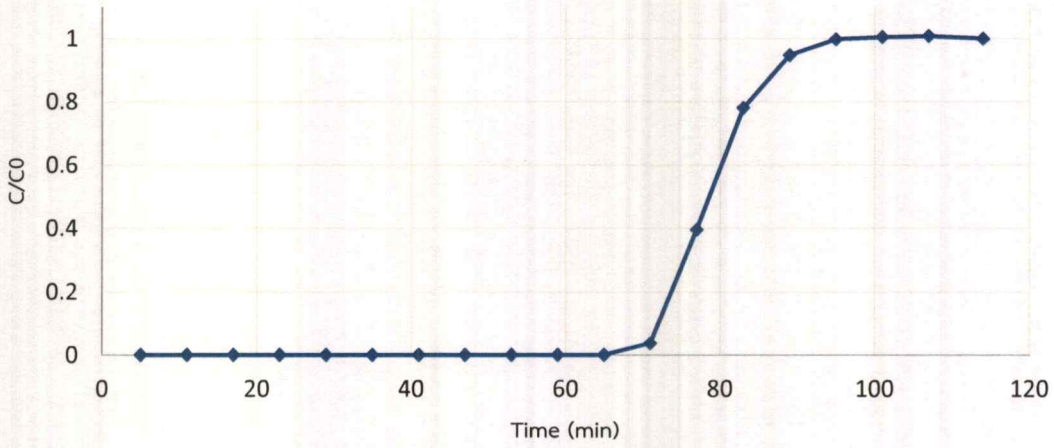

Figure C.14 Breakthrough curve of Zeolite-PVA JP-27 95% EtOH, pack 8 cm, feed 2 ml/h, N_2 flow 10 ml/min (repeat 1, 60 min desorption)

Table C.14 Breakthrough curve of Zeolite-PVA JP-27 95% EtOH, pack 8 cm, feed 2 ml/h, N_2 flow 10 ml/min (repeat 1, 60 min desorption)

	% Area water	Time	% Water	C/C0
Initial	14.761	-	5.334875	1
1	0	5	0	0
2	0	11	0	0
3	0	17	0	0
4	0	23	0	0
5	0	29	0	0
6	0	35	0	0
7	0	41	0	0
8	0	47	0	0
9	0	53	0	0
10	0	59	0	0
11	0	65	0	0
12	0.543	71	0.196256	0.036787
13	5.836	77	2.109296	0.395379
14	11.504	83	4.157872	0.779376
15	13.975	89	5.050961	0.946782
16	14.726	95	5.322394	0.997661

Table C.14 Continue

17	14.83	101	5.359983	1.004706
18	14.874	107	5.375885	1.007687
19	14.754	114	5.332514	0.999557

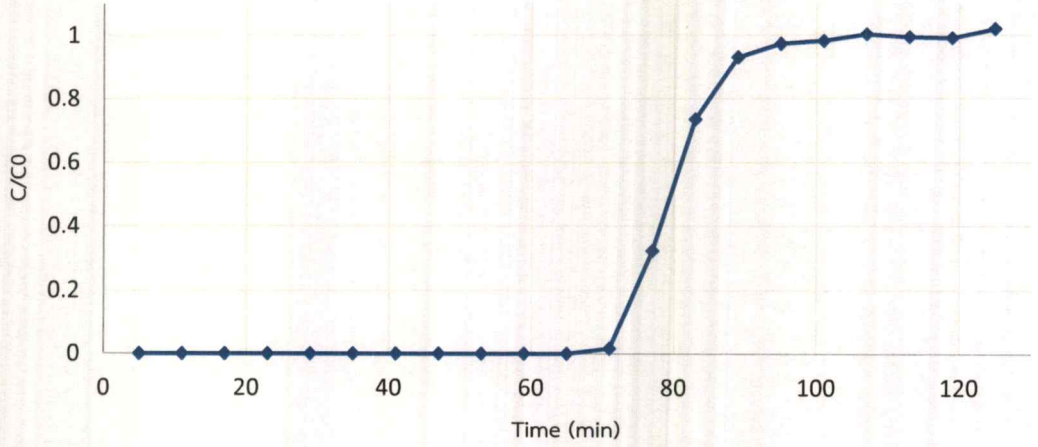

Figure C.15 Breakthrough curve of Zeolite-PVA JP-27 95% EtOH, pack 8 cm, feed 2 ml/h, N_2 flow 10 ml/min (repeat 2, 60 min desorption)

Table C.15 Breakthrough curve of Zeolite-PVA JP-27 95% EtOH, pack 8 cm, feed 2 ml/h, N_2 flow 10 ml/min (repeat 2, 60 min desorption)

	% Area water	Time	% Water	C/C0
Initial	14.233	-	5.14421	1
1	0	5	0	0
2	0	11	0	0
3	0	17	0	0
4	0	23	0	0
5	0	29	0	0
6	0	35	0	0
7	0	41	0	0
8	0	47	0	0
9	0	53	0	0
10	0	59	0	0
11	0	65	0	0
12	0.233	71	0.084321	0.016391
13	4.587	77	1.657872	0.322279
14	10.457	83	3.779456	0.734701
15	13.254	89	4.790372	0.931216
16	13.852	95	5.006506	0.973231

Table C.15 Continue

17	13.984	101	5.054214	0.982505
18	14.287	107	5.163727	1.003794
19	14.155	113	5.116019	0.994520
20	14.106	119	5.098164	0.991049
21	14.521	125	5.248301	1.020235

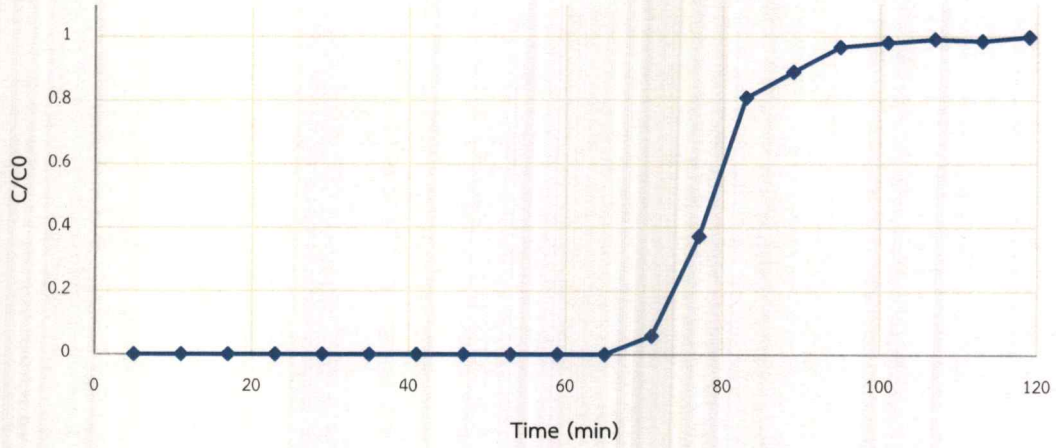

Figure C.16 Breakthrough curve of Zeolite-PVA JP-27 95% EtOH, pack 8 cm, feed 2 ml/h, N_2 flow 10 ml/min (repeat 3, 60 min desorption)

Table C.16 Breakthrough curve of Zeolite-PVA JP-27 95% EtOH, pack 8 cm, feed 2 ml/h, N_2 flow 10 ml/min (repeat 3, 60 min desorption)

	% Area water	Time	% Water	C/C0
Initial	14.502	-	5.241434	1
1	0	5	0	0
2	0	11	0	0
3	0	17	0	0
4	0	23	0	0
5	0	29	0	0
6	0	35	0	0
7	0	41	0	0
8	0	47	0	0
9	0	53	0	0
10	0	59	0	0
11	0	65	0	0
12	0.845	71	0.305407	0.058268
13	5.427	77	1.961472	0.374224
14	11.699	83	4.228350	0.806716
15	12.875	89	4.653390	0.887809
16	14.012	95	5.064334	0.966212

Table C.16 Continue

17	14.214	101	5.137343	0.980141
18	14.355	107	5.188304	0.989863
19	14.282	113	5.161920	0.984830
20	14.457	119	5.225170	0.996897

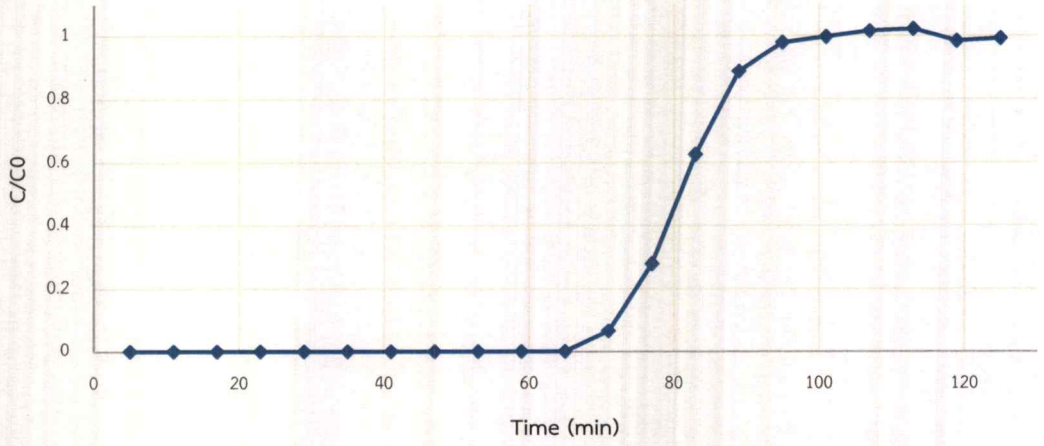

Figure C.17 Breakthrough curve of Zeolite-PVA JP-27 95% EtOH, pack 8 cm, feed 2 ml/h, N_2 flow 10 ml/min (repeat 4, 60 min desorption)

Table C.17 Breakthrough curve of Zeolite-PVA JP-27 95% EtOH, pack 8 cm, feed 2 ml/h, N_2 flow 10 ml/min (repeat 4, 60 min desorption)

	% Area water	Time	% Water	C/C0
Initial	12.444	-	4.497521	1
1	0	5	0	0
2	0	11	0	0
3	0	17	0	0
4	0	23	0	0
5	0	29	0	0
6	0	35	0	0
7	0	41	0	0
8	0	47	0	0
9	0	53	0	0
10	0	59	0	0
11	0	65	0	0
12	0.808	71	0.292034	0.064932
13	3.483	77	1.258855	0.279900
14	7.792	83	2.816250	0.626178
15	11.054	89	3.995229	0.888318
16	12.185	95	4.404005	0.979207

Table C.17 Continue

17	12.405	101	4.483519	0.996887
18	12.637	107	4.567370	1.015531
19	12.716	113	4.595923	1.021879
20	12.240	119	4.423883	0.983627
21	12.347	125	4.462556	0.992226

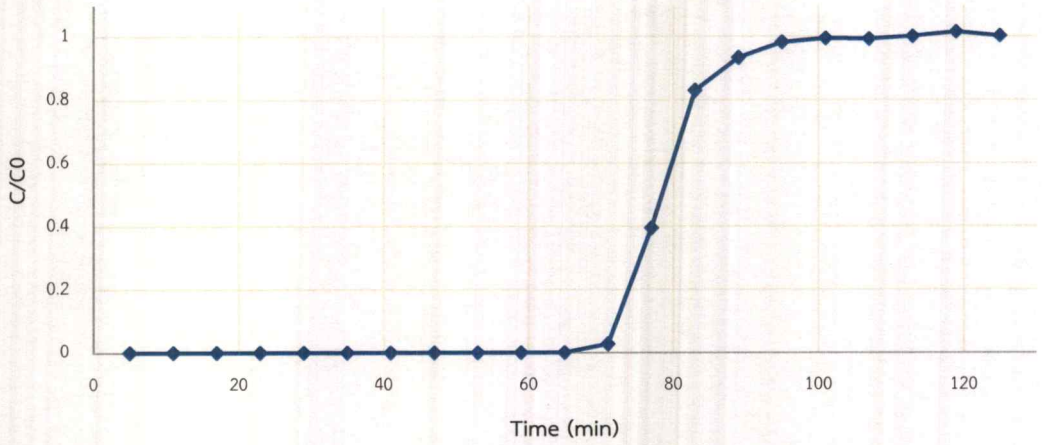

Figure C.18 Breakthrough curve of Zeolite-PVA JP-27 95% EtOH, pack 8 cm, feed 2 ml/h, N_2 flow 10 ml/min (repeat 5, 60 min desorption)

Table C.18 Breakthrough curve of Zeolite-PVA JP-27 95% EtOH, pack 8 cm, feed 2 ml/h, N_2 flow 10 ml/min (repeat 5, 60 min desorption)

	% Area water	Time	% Water	C/C0
Initial	11.617	-	4.198745	1
1	0	5	0	0
2	0	11	0	0
3	0	17	0	0
4	0	23	0	0
5	0	29	0	0
6	0	35	0	0
7	0	41	0	0
8	0	47	0	0
9	0	53	0	0
10	0	59	0	0
11	0	65	0	0
12	0.318	71	0.114934	0.027373
13	4.596	77	1.661125	0.395624
14	9.639	83	3.483808	0.829726
15	10.836	89	3.916438	0.932764
16	11.407	95	4.122813	0.981916

Table C.18 Continue

17	11.551	101	4.174859	0.994311
18	11.531	107	4.167630	0.992590
19	11.628	113	4.202689	1.000939
20	11.798	119	4.264132	1.015573
21	11.648	125	4.209918	1.002661